THE IMPROVEMENT OF HYDROGEN LOADING TIME TO FIBER BRAGG GRATING FABRICATION PRODUCTIVITY IMPROVEMENT

Phimolphan Rutthongjan

A Thesis Submitted in Partial Fulfillment of Requirements
for the Degree of Master of Engineering Program in Engineering Technology
Graduated School
Thai-Nichi Institute of Technology
Academic Year 2015

Thesis Title	The improvement of hydrogen loading time to fiber Bragg grating fabrication productivity improvement
By	Phimolphan Rutthongjan
Field of Study	Engineering Technology
Advisor	Dr. Phaisarn Sudwilai

The Graduate School of Thai-Nichi Institute of Technology has been approved and accepted as partial fulfillment of the requirements for the Master's Degree

…………………………..…………….. Dean of Graduate School
(Assoc. Prof. Dr. Pichit Sukchareonpong)
Month.…..…..… Date…….., Year……...…..

Thesis Committees

…………………………..…………….. Chairperson
(Dr. Surapong Pongyupinpanich)

…………………………..…………….. Committee
(Asst. Prof. Dr. Wimol San-um)

…………………………..…………….. Committee
(Asst. Prof. Dr. Warakorn Srichavengsup)

…………………………..…………….. Advisor
(Dr. Phaisarn Sudwilai)

PHIMOLPHAN RUTTHONGJAN: THE IMPROVEMENT OF HYDROGEN LOADING TIME TO FIBER BRAGG GRATING FABRICATION PRODUCTIVITY IMPROVEMENT. ADVISOR: DR. PHAISARN SUDWILAI, 63 PP.

FBG fabrication technology has been quickly developed. The optical communication business is highly competitive. The FBG productivity improvement is an optional to drive on this business. The motivation of this research is to improve the cycle time of hydrogen loading process from hydrogen loading time reduction for improve FBG productivity. The objective of hydrogen loading process is to enhance photosensitivity of fiber. However, the side effect of this process is to increase the refractive index of fiber core. These two effects of hydrogen affect to the quality of FBG. Therefore, in this research was studied the effect of hydrogen loading time to FBG parameter. Hydrogen pressure was controlled at 13 MPa. Hydrogen loading time were varied at 48, 72, 120, and 192 hours. The standard deviation of FBG parameter were considered to be a judgment factor. All of hydrogen loading time were accepted by judgment from the standard deviation of each FBG parameter. However, the average of writing time in case of hydrogen loading time at 48 hours was fluctuation more than 72 hours. Therefore, Hydrogen loading time at 72 hours was the best of hydrogen loading time that can improve FBG productivity, as well as, sustain a quality of FBG.

Graduated School	Student’s Signature……………………
Field of Engineering Technology	Advisor’s Signature……………………
Academic Year 2015	

Acknowledgement

I would like to thank my company that support the equipment and material for experiment testing. My co-worker who always support me and share the knowledge with me. I am also sincerely thankful to my advisor, Dr. Phaisarn sudwilai for his suggestion for my thesis. Thesis committee, Asst. Prof. Dr. Wimol-sanum, Assr. Prof Dr. Warakorn Srichavengsup, and Dr. Surapong Pongyupinpanich for their comment to improve my thesis.

Finally, I would like to thank my mother who always support me for everything. My friend at MET-02 and MET-03 who make me enjoy during study at Thai-Nichi institute of Technology.

Phimolphan Rutthongjan

Table of Contents

Pages

Chapter

Table of Contents (Continued)

Table of Contents (Continued)

Chapter **Pages**

Table of Contents (Continued)

List of Table

List of Figures

List of Figures (Continued)

Figures **Pages**

List of Figures (Continued)

List of Figures (Continued)

Chapter 1

Introduction

1.1 Background and problems

Fiber Bragg Grating (FBG) is a periodic change of refractive index of fiber core by UV radiation. In 1978, FBG was discovered by Kan Hill and co worker in Canada. There are several applications of FBG in several fields of industry. Fiber amplifier, Fiber filter, and Dispersion compensator are used in optical telecommunication. Strain sensor, Temperature sensor, Chemical sensor, and Accelerometerers are used in Sensors device. Welding metal and cut metal manufacturing by Fiber laser.

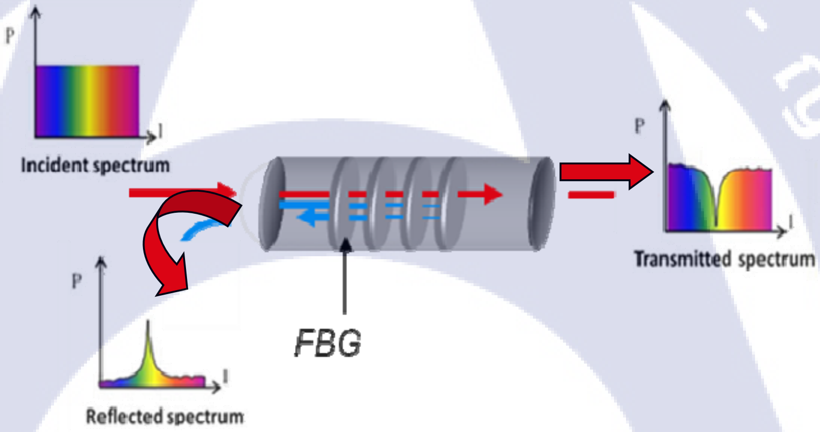

Figure 1.1 The schematic of reflected spectrum and transmitted spectrum when incident spectrum travel through fiber Bragg grating.

When the board and multi wavelength light travel through an FBG, there are some light at specific wavelength will be reflected from FBG. The specific wavelength is depended on FBG pitch. Another effect is the rest of light that except the reflected spectrum will pass through the FBG. This is a transmitted spectrum as shown in Figure1.1.

In this research, the reflected spectrum is used for study. The important parameters of reflected spectrum are FBG wavelength, Reflectivity, and Bandwidth as show in Figure1.2.

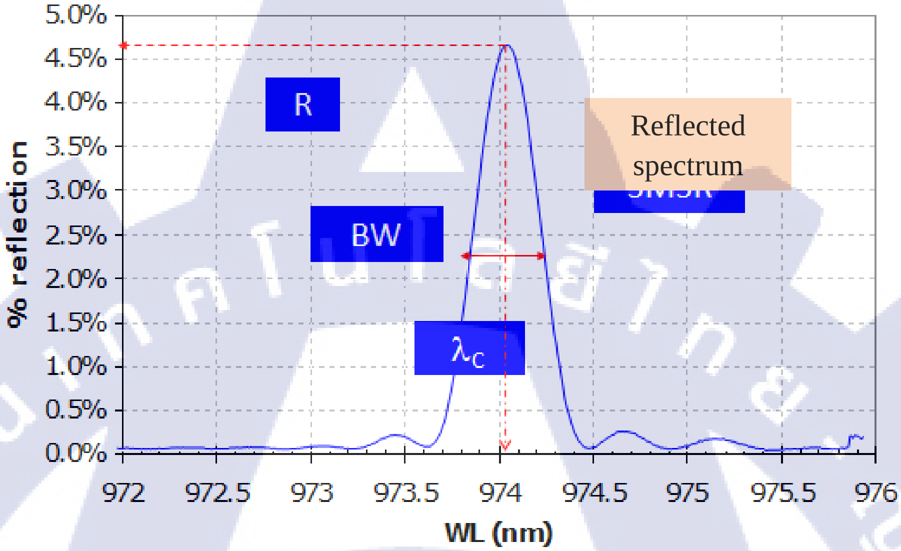

Figure 1.2 The important parameters of FBG reflected spectrum

Recently, optical communication business has a high competitive that include Fiber Bragg Grating manufacturing. To drive on this business, the productivity improvement is an optional. The FBG fabrication process flow is consisted of five important processes. Start by enhance photosensitivity of fiber by hydrogen loading process. To inscribe FBG on fiber from UV laser with phase mask technique by writing process. Stabilize FBG by thermal stabilization process. To enhance FBG strength by FBG recoating process. Hydrogen annealing process for elimination hydrogen gas in fiber. Finally, measure FBG parameter at optical inspection process. These processes as show in Figure1.3.

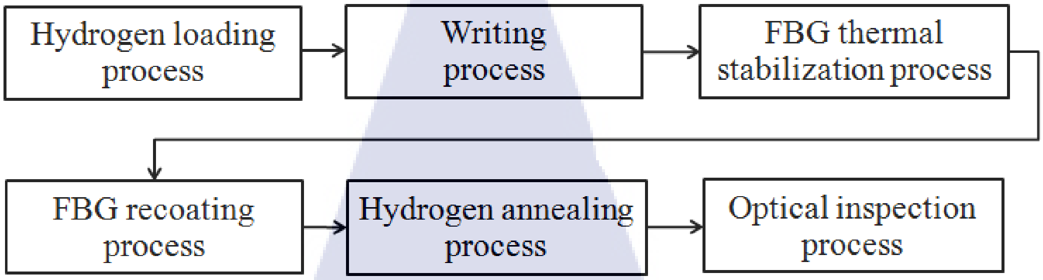

Figure 1.3 The FBG fabrication process flow

From these all process, hydrogen loading process is a process that consumes the highest of cycle time. The cycle time unit of hydrogen loading process is day. In contract, the cycle time unit of the other processes are minute.

On this research, Researcher would like to improve FBG fabrication productivity by improvement hydrogen loading time of hydrogen loading process. Due to the main purpose of hydrogen loading process is to enhance photosensitivity of fiber core. This advantage of photosensitivity is developed to improve the writing time at FBG writing process. However, FBG wavelength shift to shorter wavelength when hydrogen diffuse from FBG that is a side effect of hydrogen loading process. Writing time and FBG wavelength shift such an important factors of FBG reflected spectrum. Therefore, to finding the optimized condition of hydrogen loading time. The effect of hydrogen to FBG parameter is necessary for studying.

1.2 Research objectives

1.2.1 Study the effect of hydrogen concentration in fiber to FBG important parameters.

1.2.2 Finding Hydrogen loading time to improve FBG productivity, as well as, sustain a quality of FBG.

1.3 Scope of the thesis

This thesis study effects of Hydrogen concentration to FBG important parameter in case of FBG wavelength, FBG reflectivity and FBG bandwidth. Grating type is uniform grating.

1.3.1 The Hydrogen concentration will be controlled by varying hydrogen loading time conditions (48, 72, 120, and 192 days). Hydrogen pressure is controlled at 13 MPa.

1.3.2 FBG wavelength range is 980 nm and 1480 nm. FBG reflectivity less than 4% and 1 % at optical inspection process for 980 and 1480 respectively.

1.3.3 Single mode fiber (SMF) is a material for FBG wavelength range are 980 nm. and Polarization-Maintaining single mode fiber (PMF) is a material for FBG wavelength range 1480 nm.

1.3.4 Hydrogen absorption at 1240 nm technique is used for evaluation hydrogen concentration in fiber.

1.4 Research advantage

1.4.1 We can understand the effect of hydrogen concentration in fiber core at various of hydrogen loading time to FBG parameters.

1.4.2 We can improve productivity of FBG fabrication as well as, sustain a quality of FBG.

Chapter 2

Fundamental theory and literatures review

2.1 Fundamental theory

The chapter 2 present fundamental theory, fiber optic introduction, hydrogen loading process, photosensitivity in fiber, hydrogen absorption technique, and The method to inscribe FBG. Literature reviews emphasize to the effect of hydrogen to FBG wavelength shift, Hydrogen absorption loss technique.

2.1.1 Fiber optic introduction [1].

Fiber optic technology was started in 1790, to the optical semaphore telegraph invented by French inventor Claude Chappe. Fiber optic technology was developed by many of researcher. Until in the summer of 1970, one team of researchers began experimenting with fused silica, a material capable of extreme purity with a high melting point and a low refractive index. Corning Glass researchers Robert Maurer, Donald Keck, and Peter Schultz invented fiber-optic wire or "optical waveguide fibers" (patent no. 3,711,262), which was capable of carrying 65,000 times more information than copper wire, through which information carried by a pattern of light waves could be decoded at a destination even a thousand miles away. This discovery had a high improvement of optical telecommunications. The common structure of fiber optic is composed of three layers, first layer is core fiber which is usually made from silica, second layer is cladding, and last layer is coating polymer which can call jacket. Refractive index of fiber core is higher than the refractive index of cladding as show in Figure2.1. The refractive index of core increasing can do by doping technique. The generally dopants is germanium. From the different of refractive of both areas, light total internal reflection at core and cladding boundaries that affect to a little attenuation loss of light travel through the fiber optic for tens kilometers on 1550 nm wavelength region.

The schematic idea of the optical fiber transmission is shown in Figure 2.2. The advantage of optical fiber transmission is to immense binary flow rates, of the order of several Tb/s, under laboratory conditions reaching the order of 10 Tb/s, impossible while using copper based media. Low attenuation, the signal can be transmitted over long distances without regeneration.

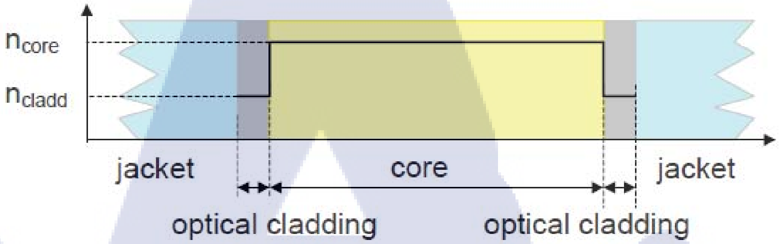

Figure 2.1 Refractive index profile of silica glass fiber [2]

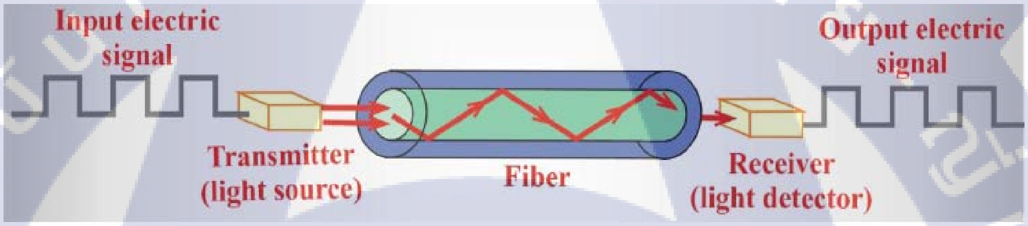

Figure 2.2 Schematic representation of fiber optics system [3]

2.1.2 Fiber optics types [3]

Optical fiber can be divided into various types. In this research is presented fiber type that considering the number of propagation mode. It can divide optical fibers into single-mode or multimode fibers. **Multimode fibers (MMF)** are characterized by a large core diameter (50 or 62.5 µm). **Single mode fiber (SMF)** are characterized by a large core diameter (from 5 to 10 µm). The cladding diameter in both fiber type is 125 µm. The Dimension of the multimode fiber and single mode fiber as shown in Figure 2.3

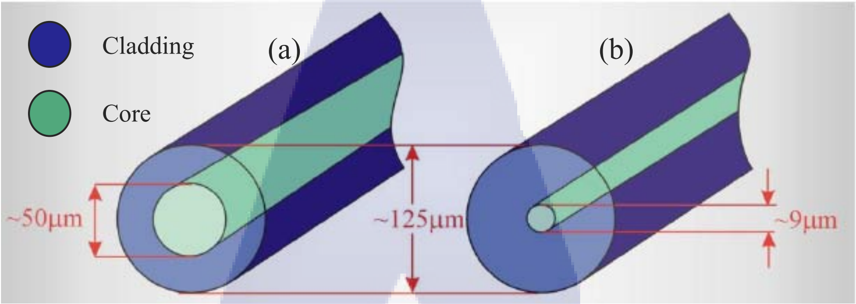

Figure 2.3 Dimension of the multimode fiber (a) and the single mode fiber (b) [3]

The technologies of fiber have been developed. Polarization maintaining optical fiber (PM) is a single mode fiber which use in some applications maintaining constant polarization of light in an optical fiber.

In polarization maintaining (PM) fiber, in which birefringence was intentionally created, polarization state does not change chaotically. The distinguished optical axis causes that random changes of density fluctuation and temporary changes of optical axis become negligible and are masked by main effect - intentionally created birefringence. When the light polarization coincides with optical axis (or the axis parallel to it) polarization state does not change over long distances. However, if the optical axis is at an angle to polarization direction, two orthogonal components are created: slow (in negative crystal it corresponds to an extraordinary beam) and fastbeam (ordinary), which, for longer optical distances, generate periodically changing phase difference. Thus, for 45º angle, first we observe linear polarization, followed by elliptical and circular polarization (with phase difference $\Delta\Phi = \frac{\Pi}{2}$**),** subsequently again linear ($\Delta\Phi = \Pi$), but perpendicular to the linear polarization at entrance, elliptical, circular ($\Delta\Phi = \frac{3\Pi}{2}$), in order to return to initial polarization after a full period ($\Delta\Phi = 2\Pi$) For longer distances the cycle repeats. Figure 2.4 shows the evolution of polarization state in polarization maintaining fiber, in case when the input signal is linearly polarization at 45º from a slow optical axis.

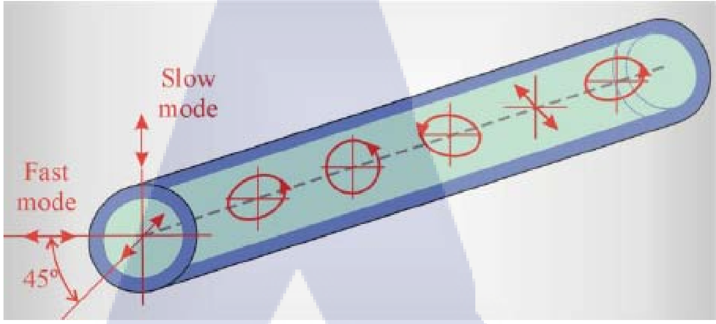

Figure 2.4 Evolution of state of polarization along a polarization maintaining fiber, when the input signal is linearly polarized at 45º from the slow axis [3]

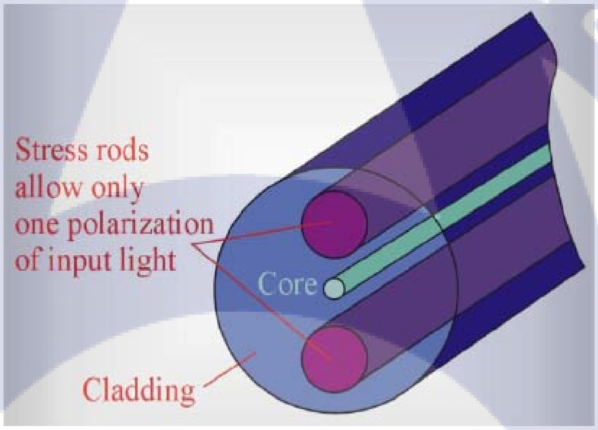

Figure 2.5 Cross-section of polarization maintaining fiber [3]

2.1.2.1 Propagation of light in optical fibers. Electrodynamics Analysis. (Step-index Cylindrical fiber) [3]

Propagation of light in optical fibers is described by Maxwell equations, similarly to all other electromagnetic phenomena. The wave equation derived from the Maxwell equations describes propagation of light in optical fiber. If make the following assumptions, nonlinear polarization is negligible, it can neglect the imaginary component of dielectric constant, $\varepsilon(\omega)=\left(n(\omega)+i\alpha c\right)/2\omega)^2$, because the loss in optical fiber is low in spectrum range of interest for fiber optics techniques, therefore $\alpha \approx 0$, refractive index does not depend on core and cladding spatial coefficients, then the wave equation takes form of equation known as Helmholtz equation

$$\nabla^2 \overline{E} + n^2(\omega) k_0^2 \overline{E} = 0 \tag{2.1}$$

In Cartesian coordinate system Laplace operator is expressed as follows: (1.13)

$$\nabla^2 = \frac{\partial^2}{\partial x^2} + \frac{\partial^2}{\partial y^2} + \frac{\partial^2}{\partial z^2} \tag{2.2}$$

where $k_0 = \frac{\omega}{c} = \omega\sqrt{\mu_0 \varepsilon_0}$ is the wave vector length (wave number), μ_0 and ε_0 denote magnetic and dielectric permeability of free space, $\overline{E} = \overline{E}(r, \omega)$ is Fourier transform of electric field

$$\overline{E}(r,\omega) = \int_{-\infty}^{+\infty} E(r,t) \exp(i\omega t) dt \tag{2.3}$$

Propagation of light and mode analysis is described in details in numerous handbooks . It can consider the solution of equation (2.1). Equation (2.1) is a vector equation, therefore it is an equivalent of three differential scalar equation for three electric field **E** components. In Cartesian coordinate system those are *Ex, Ey, Ez* and this description is most proper for planar waveguides . For optical fibers, most commonly used in telecommunications, it is most convenient to use polar coordinates (r, ϕ, z) because of cylindrical symmetry of optical fibers. Then, Equation (2.1) takes the following form this below equation

$$\frac{\partial^2 \overline{E}}{\partial r^2} + \frac{1}{r}\frac{\partial^2 \overline{E}}{\partial r^2} + \frac{1}{r^2}\frac{\partial^2 \overline{E}}{\partial \phi^2} + \frac{\partial^2 \overline{E}}{\partial z^2} + n^2 k_0^2 \overline{E} = 0 \tag{2.4}$$

Cartesian and polar coordinates are linked as follows $x = r\cos\phi, y = \cos\phi, z = z$ Similar equation can be written for magnetic field strength $\boldsymbol{H}$. Full solution must therefore contain six components, however, taking into account four Maxwell equations, only two components are independent. Let us choose $\overline{E_z}$ and $\overline{H_z}$ independent components. Assuming that the *z* axis overlaps with optical fiber axis, we obtain the following scalar equation for electric field E_z component along the fiber axis

$$\frac{\partial^2 \overline{E}}{\partial r^2} + \frac{1}{r}\frac{\partial^2 \overline{E_z}}{\partial r^2} + \frac{1}{r^2}\frac{\partial^2 \overline{E_z}}{\partial \phi^2} + \frac{\partial^2 \overline{E_z}}{\partial z^2} + n^2 k_0^2 \overline{E_z} = 0 \tag{2.5}$$

Of course, the fact, that the electric field component E_z is directed along the fiber axis does not imply that the electromagnetic wave seizes to be a transverse wave. The wave propagating in a fiber can show any polarization, which can be depicted as superposition of waves having their vectors in two mutually perpendicular planes (denoted as *s* and *p* polarization). Transverse magnetic (TM) waves, which electric field vector shows *s* polarization are characterized with non-zero electric field intensity $E_z \neq 0$, along the fiber axis *z*, whilst magnetic field component $H_z = 0$. On the contrary, in the case of transverse electric (TE) waves, electric field vector shows *p* ,$E_z = 0$, whilst $H_z \neq 0$, .

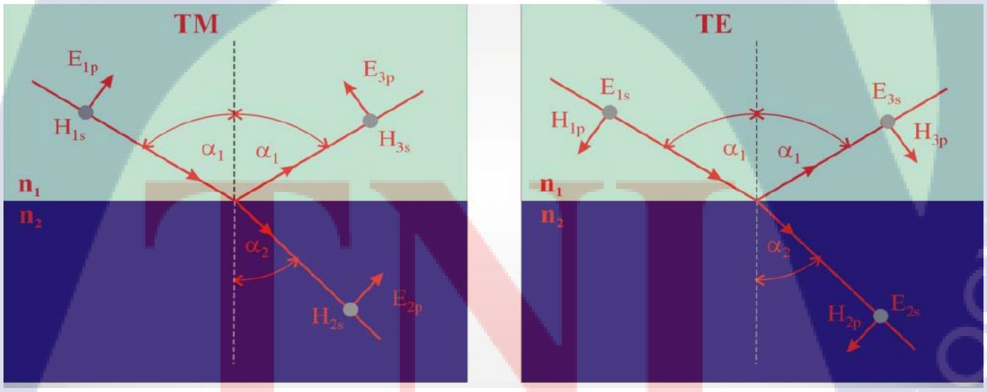

Figure 2.6 Illustration of TM and TE modes. Index p denotes electric field intensity vector in the plane incorporating fiber axis, s – perpendicular to this plane [3]

It can apply the method of variable separation to solve the equation (2.5). It will be looking for the solution in a form

$$\overline{E_z} = R(r)\Phi(\phi)Z(z) \tag{2.6}$$

Substituting equation (2.6) to (2.5) and dividing both sides of equation (2.5) by

$$R(r)\Phi(\phi)Z(z) \tag{2.7}$$

$$\frac{1}{z}\frac{d^2Z}{dz^2} = -\left(\frac{1}{R}\frac{d^2R}{dr^2} + \frac{1}{Rr}\frac{dR}{dr} + \frac{1}{r^2\Phi}\frac{d^2\Phi}{d\phi^2} + n^2k_0^2\right) \tag{2.8}$$

It can be seen, right side of the equation does not depend on *z*, therefore the changes along fiber axis *z* do not influence the right side of the equation. This means, that the left side of the equation must be a certain constant (in general, a complex constant). It can denote this constant as γ^2 where

□□
□□□□□□□□

$\gamma = \alpha + i\beta$ □□□□□□□□□□□□□□□□□□□□□□□□□□□□□□□□□□□□□□
□□□□□□□□□□ (2.9)

It expect the solution of equation in form of oscillating wave, therefore □□must denote phase constant and is named propagation constant, while □□describes
attenuation (and oscillating wave fading away) in optical fiber. As the attenuation in optical fiber is low, It can assume with good approximation $\alpha = 0$.

$$\frac{1}{z}\frac{d^2Z}{dz^2} = \gamma^2 \tag{2.10}$$

The solution of equation (2.10) is well known function

$$Z(z) = C_1\exp(-\gamma z) + C_2\exp(\gamma z) \tag{2.11}$$

representing waves propagating in opposite directions along the fiber axis, where C_1 and C_2 are the constants determined from boundary conditions. In further discussion we will consider only the wave propagating in the positive direction, making the assumption $C_2=0$. Solving the right side of equation (2.8). it obtain

$$\frac{1}{\Phi}\frac{d^2\Phi}{d\phi^2} = -(\frac{r^2}{R}\frac{d^2R}{dr^2} + \frac{r}{R}\frac{dR}{dr} + r^2\gamma^2 + r^2n^2k_0^2) \tag{2.12}$$

Right side of this equation does not depend on □, thus the left side of the equation must be equal to a certain constant, which it will denote as $-m^2$. Therefore It obtain

$$\Phi(\phi) = C_3\cos(m\phi) + C_4\sin(m\phi) \tag{2.13}$$

where C_3 and C_4 are the constants determined from boundary conditions. Function $\Phi(\phi)$ must meet the condition of rotational symmetry, $\Phi(\phi) = \Phi(\phi + 2\Pi)$, therefore m in equation 2.13 must be an integer. Finally, substituting γ^2 □and m^2 constants into equation 2.8 it obtain.

$$\frac{d^2R}{dr^2} + \frac{1}{r}\frac{dR}{dr} + (h^2 - \frac{m^2}{r^2})R = 0 \tag{2.14}$$

Where $h^2 = \gamma^2 + n^2k_0^2$ The solution of equation 2.24 should exhibit oscillatory character in the core and decaying in the cladding. In order for this condition to be met, h must be a real number in the core, and imaginary number in the cladding, that is: h □□h_1 for $r<a$.

The solution for ordinary differential equation 2.14 and 2.15 for h □□h_1 , that is in the core, are Bessel functions.

$$R(r) = C_5J_m(h_1r) + C_6N_m(h_1r) \qquad \text{for } r<a \tag{2.15}$$

Function J_m is a Bessel function of the first kind, N_m is a Bessel function of the second kind and m order and is called Neumann function. Figures 2.7 and 2.8 depict Bessel functions of first and second kind. For $r \rightarrow 0$ N_m function approach minus infinity, and has no physical meaning. It was avoided only if it was assumed that C_6=0.

$$r\overline{E_z} = J_m(h_1 r)(A_1 \cos m\phi + B_1 \sin m\phi)\exp(-\gamma z) \qquad r<a \tag{2.16}$$

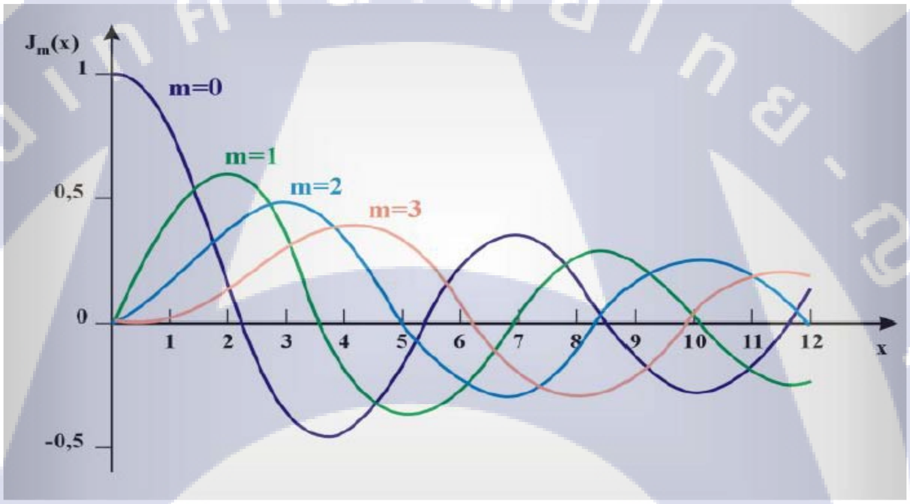

Figure 2.7 Bessel function of the first kind and m order [3]

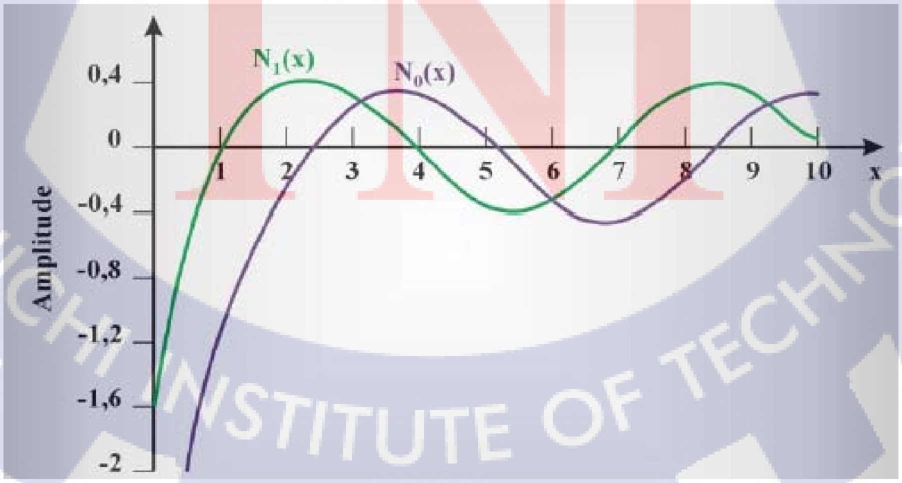

Figure 2.8 Bessel function of the second kind and m order [3]

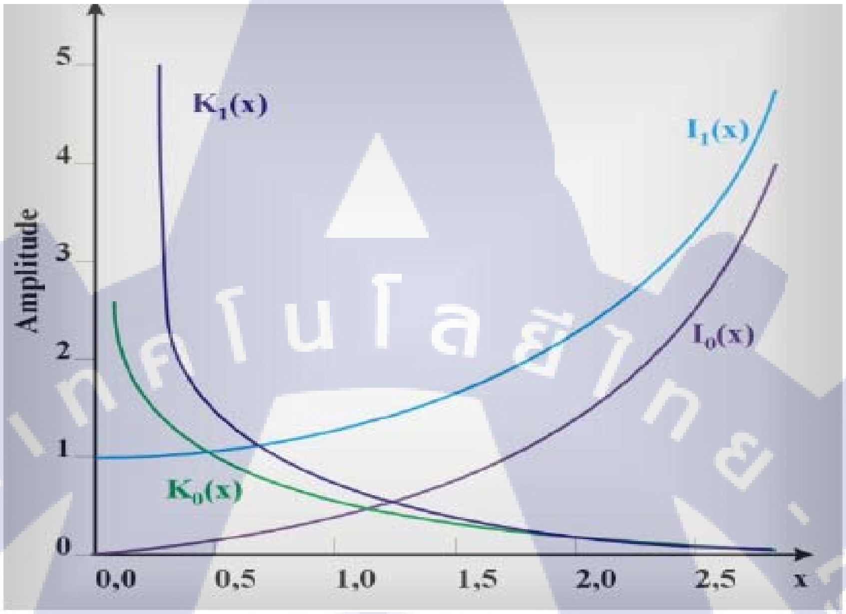

Figure 2.9 Modified Bessel function of the first and the second kind and m order [3]

Using the denotation (2.15) Bessel equations (2.14) for the core takes form

$$\frac{d^2R}{dr^2}+\frac{1}{r}\frac{dR}{dr}-(h_2^2+\frac{m^2}{r^2})R=0 \qquad r>a \tag{2.17}$$

and its solution is

$$R(r)=C_7I_m(h_2r)+C_8K_m(h_2r) \tag{2.18}$$

Function I_m is a modified Bessel function of the first kind, function K_m is a modified

Bessel function of the second kind and *m* order. Figure. 2.9 shows Bessel functions of the first and the second kind. For *r*□□□□*m N* function approach infinity, and has no physical meaning.

2.1.3 Fiber Bragg Grating introduction [4]

Fiber Bragg Grating was discovered by Ken Hill *et al*. He use argon ion laser to expose the light pass through Germania-doping silica fiber. The refractive index of fiber core was increased from that experiment. Therefore, the periodic refractive index change is the Fiber Bragg Grating. There are two phenomenons when light from multi wavelength pass through FBG. First phenomenon is reflected spectrum at specific wavelength. Reflected wavelength is depended on refractive index change of FBG area. Another phenomenon is the rest of light that not include reflected wavelength that is called transmitted spectrum. On this research, reflected spectrum is studied. The important parameters of reflected spectrum FBG consist of four parameters. Wavelength, reflectivity, bandwidth, and side mode suspension ration. FBG wavelength given by Bragg wavelength (λ_B) as follow equation (2.19) [4].

$$\lambda_B=2n_{eff}\Lambda \qquad (2.19)$$

where n_{eff} is the modal index and is the grating period. Each reflection from a crest in the index perturbation is in phase with the next one at , as shown in Figure2.10, and any change in fiber properties, such as strain, temperature, or polarization which varies the modal index or grating pitch will change the Bragg wavelength.

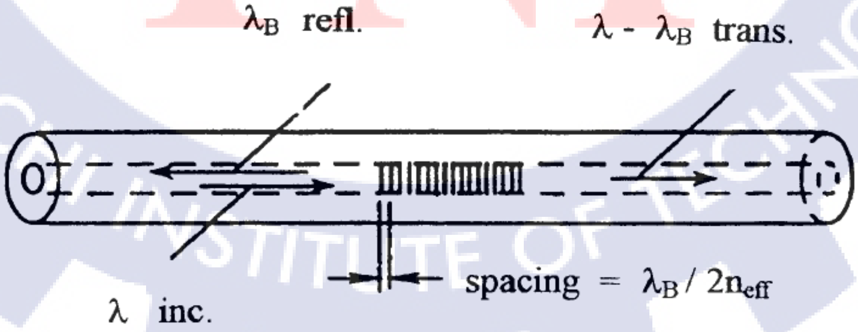

Figure 2.10 A schematic of refractive index pattern of fiber Bragg grating [4].

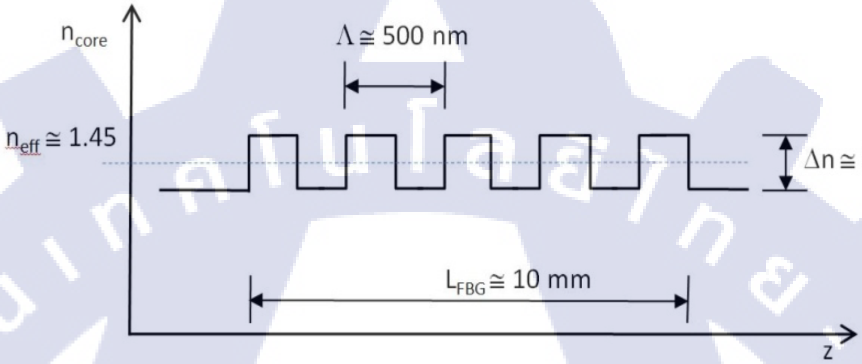

Figure 2.11 The schematic of the changing of refractive index of FBG [5].

Reflectivity is an important parameter of FBG. The definition of reflectivity is expressed by equation (2.20) [6].

$$|\rho|^2 = \tanh^2(KL) \tag{2.20}$$

Where $|\rho|^2$ is reflectivity, K is coupling coefficient, and L is grating length. K is defined by equation (2.21).

$$K = \frac{4\prod \eta \Delta n}{\lambda_b} \tag{2.21}$$

Where η is an Eta, Δn is refractive index change as shown in Figure2.11, and λ_b is Bragg wavelength.

The definition of FBG bandwidth is expressed by equation (2.22).

$$\Delta\lambda = \frac{\lambda_b^{\,2}}{2\prod n_{eff} L}\sqrt{(KL)^2 + \prod^2} \qquad (2.22)$$

Where $\Delta\lambda$ is bandwidth from the peak to the first Zero, λ_b is Bragg wavelength, n_{eff} is effective index, K is coupling coefficient, and L is grating length. From equation (2.22).

2.1.4 Fiber Bragg Grating types [7].

There are several different categories of fiber Bragg gratings which result from different processes. Recently a new classification system was proposed which is based on the formation mechanism. Type I Gratings are studied on this research

2.1.4.1 Type I Gratings [7]

Type I gratings were initially formed in germanosilicate fiber, at least for small index changes, by a single UV photon absorption process that excites oxygen deficiency defect centers (ODC) with absorption bands around 244 nm. For large index changes, it is likely that defect formation is also accompanied by densification of the glass matrix.

Type I gratings exhibit a positive change in the refractive index and a temperature dependent decay which can be characterized using a power law. This decay is the result of the thermal depopulation of trapped excited states that are created during the grating formation. At elevated temperatures, carriers in the shallowest traps can absorb enough energy to escape and return to the ground state. The remaining carriers are thus associated with more stable states which can also relax to the ground state if the temperature is elevated further. As the most unstable carriers decay at lower temperatures, type I gratings are typically annealed at temperatures higher than their designed operating temperature in order to obtain long term stability in their reflectivity.

2.1.4.2 Type II Gratings [7]

Using high peak power pulsed ultraviolet laser sources, such as Krypton Fluoride-based excimer lasers, high reflectivity gratings (<99%) have been inscribed with a single laser pulse. These gratings result from a threshold dependent multiphoton ionization process similar to laser induced damage in bulk optics, hence the gratings are often referred to as ‘damage’ gratings. Such gratings are stable at temperatures over 1,000 °C and have been used to fabricate grating arrays while the fiber is being pulled on the draw tower. The single shot exposure tends to produce grating structures which can suffer from significant scattering loss. The damage like process also has the tendency to reduce the reliability and mechanical strength of the fiber.

2.1.4.3 Type IIA Gratings [7]

When UV-laser induced gratings are written in highly stressed Ge-doped core fibers, it is observed that under certain conditions, a Type I grating will grow and then decrease in strength as the grating saturates. Continued exposure results in secondary grating growth that exhibits a steady blue shift in the spectral response hence a negative refractive index change. With optimized fabrication conditions grating Type In grating structures can be fabricated that are stable up to 700 °C. The mechanism associated with the final index change is generally agreed to involve some sort of stress relief within the fiber.

2.1.4.4 Chemical Composition/Regenerated Gratings [7]

The photosensitivity required for Type I grating formation can be enhanced through a process called hydrogen loading, where the optical fiber is exposed to high pressure hydrogen gas at room temperature. Hydrogen gas permeates the glass matrix until the glass is saturated. Once the fiber is loaded, UV irradiation results in the hydrogen dissociation and the formation of Si-OH or Ge-OH defects resulting in increased levels of achievable index change. After UV inscription and out diffusion of unreacted hydrogen from the fiber, careful annealing of the grating at an elevated intermediate temperature of 600–700 °C results in interstitial diffusion of hydroxyl groups to form water molecules within the glass that become highly stable thermally. The annealing at intermediate temperatures results in the erasure of the

Type I seed grating however further heating at higher temperatures generates a new grating structure at a longer wavelength. The index modulation of this new grating is significantly less than the original seed grating by about an order of magnitude. It is stable at high temperatures however and can be repeatedly cycled to temperatures above 1,000 °C. The remnant index modulation is typically less than 10−4 which results in a low reflectivity grating if its length is less than 1 cm. Because of its low index modulation, it is less susceptible to scattering losses that are often associated with Type II gratings. Recently it was shown that hydrogen need not be present during the laser inscription of the grating but during the thermal regeneration. So it is still unclear as to what is the exact mechanism that is responsible for the process.

2.1.5 Method to inscribe FBG on fiber.

There are several methods to make FBG which lead to the varied of fiber bragg grating type. The method to make FBG such as The bulk interferometer, The phase mask, and The Lloyd mirror and prism interferometer. In this research, Phase mask technique is used for inscribing FBG on fiber.

2.1.5.1 Phase mask technique [6].

A major step toward easier inscription of fiber gratings was made possible by the application of the phase mask as a component of the interferometer. Used in transmission, a phase mask is a relief grating etched in a silica plate. The significant features of the phase mask are the grooves etched into a UV-transmitting silica mask plate, with a carefully controlled mark-space ratio as well as etch depth. The principle of operation is based on the diffraction of an incident UV beam into several orders, $m = 0, \pm1, \pm2.$ ... This is shown schematically in Figure2.12. The incident and diffracted orders satisfy the general diffraction equation, with the period Λ_{pm} of the phase-mask,

$$\Lambda_{pm} = \frac{m\lambda_{uv}}{(\sin\left(\frac{\theta_m}{2}\right) - \sin\theta_i)} \tag{2.23}$$

where $\theta_m/2$ is the angle of the diffracted order, λ_{uv} the wavelength, and θ_i the angle of the incident UV beam. In instances when the period of the grating lies between λ_{uv} and $\lambda_{uv}/2$, the incident wave is diffracted into only a single order *(m* = -1) with the rest of the power remaining in the transmitted wave *(m* = 0).

With the UV radiation at normal incidence, θ_i = 0, the diffracted radiation is split into *m* = 0 and ±1 orders, as shown in Figure 2.13. The interference pattern at the fiber of two such beams of orders ± 1 brought together by parallel mirrors has a period Λ_g related to the diffraction angle $\theta_m/2$ by

$$\Lambda_g = \frac{\lambda_{uv}}{2\sin\frac{\theta_m}{2}} = \frac{\Lambda_{pm}}{2} \tag{2.24}$$

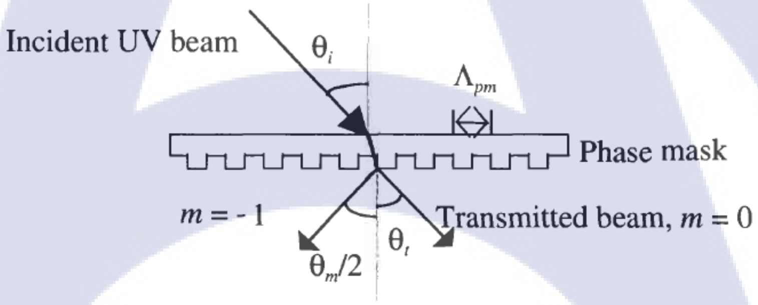

Figure 2.12 A schematic of the diffraction of an incident of an incident beam from a phase mask [6]

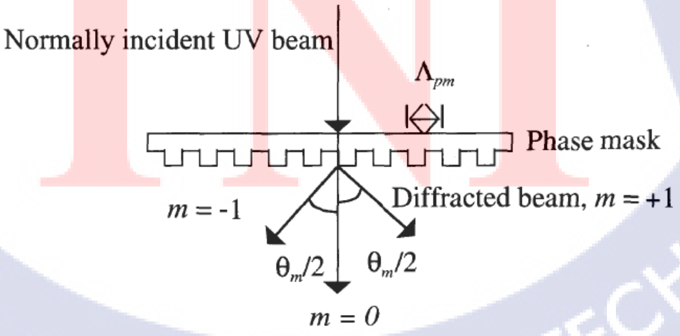

Figure 2.13 Normally incident UV beam diffracted into two ±1 orders. The remnant

radiation exits the phase-mask in the zero order *(m* = 0) [6].

The period Λ_{pm} of the grating etched in the mask is determined by the Bragg wavelength λ_{Bragg} required for the grating in the fiber and using equation (2.24) to arrive at

$$\Lambda_g = \frac{N\lambda_{Bragg}}{2n_{eff}} = \frac{\Lambda_{pm}}{2} \tag{2.25}$$

where N > 1 is an integer indicating the order of the grating period.

2.1.6 Photosensitivity in fiber optics [6].

The nature of fabrication of glass is ideally suited to promoting defects. The chemical reactions that take place in a modified chemical vapor deposition (MCVD) process are based on hot gases reacting to form a soot deposit on the inside of a silica support tube or on the outside in outside vapor phase deposition (OVD). The process allows the ratio of reactive gases such as silicon/germanium tetrachloride and oxygen to be easily changed to arrive at a nearly complete chemical reaction, depositing a mixture of germanium and silicon dioxides. It is not possible to have a 100% reaction, so the deposited chemicals have a proportion of suboxides and defects within the glass matrix. With sintering and preform collapse, these reaction components remain, although further alterations may take place while the fiber is being drawn, when bonds can break. The end result is a material that is highly inhomogeneous on a microscopic scale with little or no order beyond the range of a few molecular distances. The fabrication process also allows other higher-order ring structures to form, complicating the picture yet further. There is a possibility of incorporating not only a strained structure, but also one which has randomly distributed broken bonds and trapped defects. This is especially true of a fiber with the core dopant germanium, which readily forms suboxides as GeO *(x* = 1 to 4), creating a range of defects in the tetrahedral matrix of the silica host glass. Given this rich environment of imperfection, it is surprising that state-of-the-art germania-doped silica fiber has extremely good properties—low loss and high optical damage threshold—and is a result of better understanding of defects, which lead to increased attenuation in the transmission windows of interest. Among the well-known defects formed in the germania-doped silica core are the paramagnetic Ge(ra) defects, where *n* refers to the number of next-nearest-neighbor Ge/Si atoms surrounding a germanium ion with an associated unsatisfied single electron, first pointed out by Friebele *et al*. These defects are shown schematically in Figure 2.14. The Ge(l) and Ge(2) have been identified as trapped-electron centers. The GeE', previously known as the Ge(0) and the Ge(3) centers, which is common in oxygen-deficient germania, is a hole trapped next to a germanium at an oxygen vacancy and has been shown to be independent of the number of next-neighbor Ge sites. Here an oxygen atom is missing from the tetrahedron, while the germania atom has an extra electron as a dangling bond. The extra electron distorts the molecule of germania. The GeO defect was shown in Figure 2.14, has a germanium atom coordinated with another Si or Ge atom. This bond has the characteristic 240-nm absorption peak that is observed in many germanium-doped photosensitive optical fibers. On UV illumination, the bond readily breaks, creating the GeE' center. It is thought that the electron from the GeE' center is liberated and is free to move within the glass matrix via hopping or tunneling, or by two-photon excitation into the conduction band.

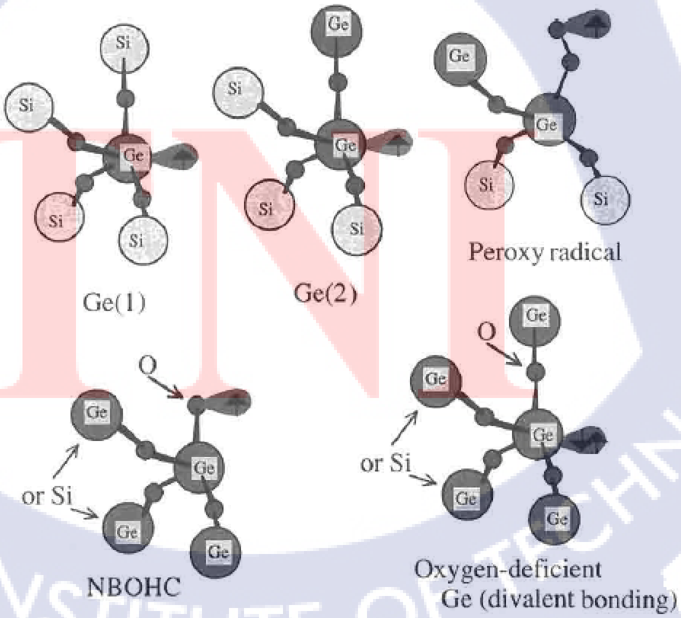

Figure 2.14 A schematic of proposed Ge (or Si) defects of germania-doped silica [6].

However, the photosensitivity is limited at 240 nm and requires shorter wavelengths, such as 193-nm radiation. Other defects include the nonbridging oxygen hole center (NBOHC), which is claimed to have absorptions at 260 and 600 nm. However, photosensitivity in fiber optic had improved from several technique such as Boron and tin as a codopant in germanosilicate fibers, hot hydrogenation and cold, high-pressure hydrogenation, and flame-assisted low-pressure hydrogen. On this research, Hydrogen loading technique is implemented to enhance photosensitivity of fiber optics.

2.1.7 Hydrogen loading technique [6].

Hydrogen loading is a general technique to enhance photosensitivity fiber for FBG fabrication. Hydrogen molecule physical bonding with fiber core when UV light expose to fiber core which lead to the dissociation of germanium-silica bonding. Therefore, Hydrogen molecule can react with silica or germanium. This effect to GeO molecules increasing that bleaching of the absorption at 240 nm partly contributes to the index change. The process may occurs as follows in Figure 2.15 (a). On the other hand, Molecular hydrogen reaction is the formation of GeH and OH ions from the defect. The GeH is responsible for the change in the refractive index via the Kramers-Kronig rule. The possible route may be show as Figure 2.15(b.)

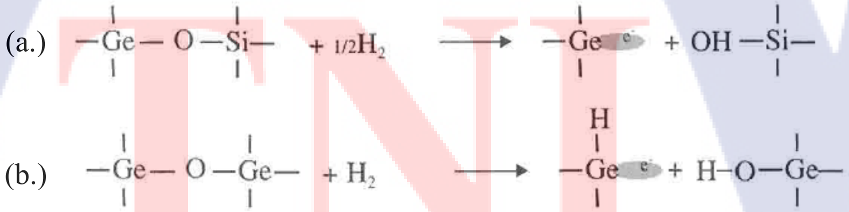

Figure 2.15 A schematic of hydrogen molecules react to germanium dope silica (a.) GeO molecules enhance photosensitivity, (b.) GeH enhance photosensitivity [6].

However, hydrogen loaded into fiber optic, this lead to loss increasing. The types of loss can be categorized into two main groups. The first group that are unreacted hydrogen and another group due to absorptive defects that form by the reaction of hydrogen with defects in the light-guiding portion of a fiber.

2.1.7.1 Losses due to unreacted hydrogen [8].

When hydrogen gas is dissolved in silica-based glasses, it appear to loss peaks in the 1070 to 1240 nm region. The effects of hydrogen on the loss spectrum of a GeO_2-doped single-mode fiber as show in Figure 2.16 , which compares representative spectra for a fiber before and after hydrogen treatment at 150°C.

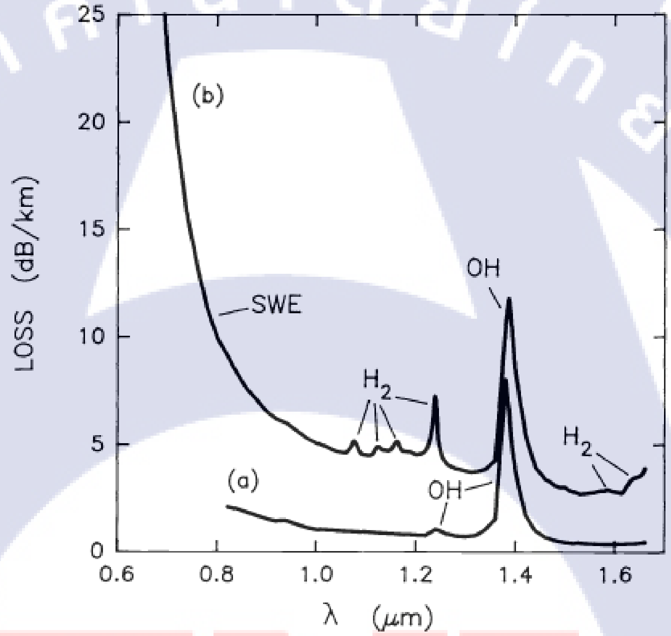

Figure 2.16 Loss spectra for a GeO_2-doped single-mode fiber, before (a) and after (b) exposure to 1 atm of H_2 at 150°C for about three days [8].

From Figure 2.16, fiber loaded hydrogen show sharp peak of hydrogen molecule on wavelength range 1070 to 1240 nm and some peak around 1600 nm that indicate from loss spectra(b). In contract, there are no any sharp peak on those wavelength from loss spectra(a). From this report, hydrogen absorption loss at 1240 nm which can use for indication the hydrogen concentration in fiber optics.

The result from Figure 2.17 shows molecular Hydrogen loss increases for a GeO_2-doped fiber exposed to high-pressure hydrogen. The magnitudes of the Hydrogen losses scale linearly with pressure, indicating a linear increase of the Hydrogen solubility with Hydrogen pressure. This loss mechanism is reversible because the Hydrogen is not chemically bonded within the glass. If the hydrogen source is removed from around the fiber, the molecular hydrogen losses will slowly diminish as the hydrogen diffuses out of the fiber.

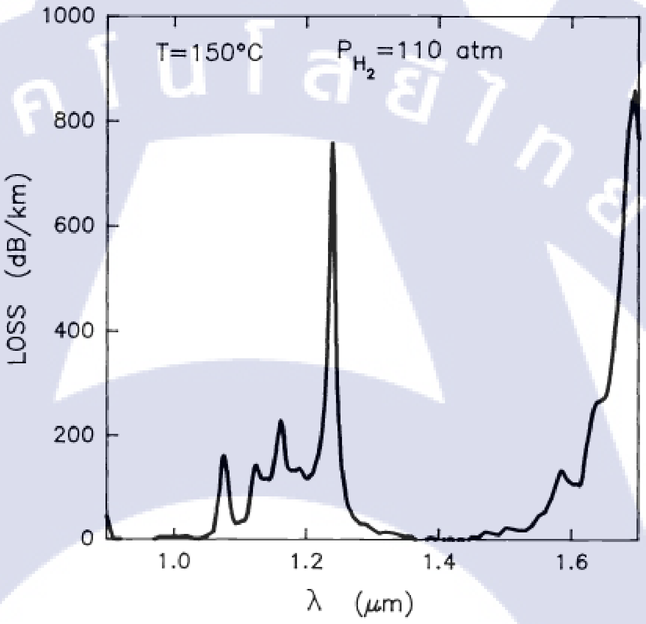

Figure 2.17 Loss increases due to molecular hydrogen dissolved in a single mode fiber at Hydrogen loading pressure 110 atm and a temperature of 150°C [8].

2.1.7.2 **Losses due to chemical reactions** [8].

In contrast to molecular hydrogen losses, there are several types of hydrogen-induced losses that are due to reactions of hydrogen at defect sites present in the light-guiding region of a fiber. These reactions generally lead to permanent loss increases .An example of such a loss change is the increase in the OH content of a fiber when it is exposed to a source of hydrogen. This can be clearly seen when the OH overtone absorption increases, around 1 .4 µm. Hydroxyl, which is bonded to silicon sites, will give rise to an overtone centered at 1.385 µm, while OH associated with germanium sites will have an absorption peak centered at about 1 .42 µm. These two types of OH growth can occur simultaneously, resulting in an overtone that is the sum of losses due to two peaks. In addition, there can be OH growth that is not so easily identified. For instance, it has been suggested that certain types of OH may be responsible for a relatively featureless long wavelength loss "edge," which is actually the wing of fundamental OH absorptions that occur at longer wavelengths, around 2.7 µm.

Hydrogen loss is the function of temperature, time, and hydrogen pressure. In this research, Hydrogen pressure was controlled and hydrogen loading temperature was assumed to same as environment temperature.

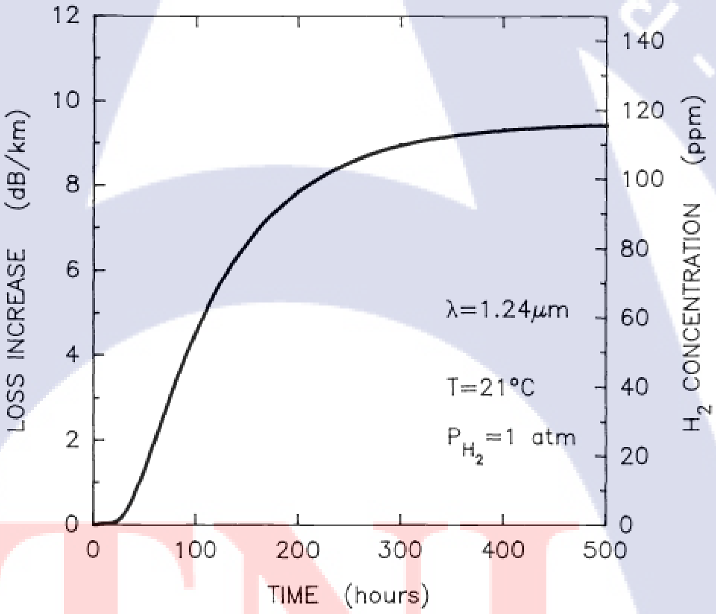

Figure 2.18 Changes in loss at 1.24 µm. due to the Hydrogen overtone as a function of time, for 21°C and hydrogen pressure 1 atm. Also shown in terms of hydrogen concentration, where 1 ppm is defined as 10^{-6} moles of Hydrogen per mole of SiO_2 [8]

Figure 2.18 shows a calculated curve for the increase in the concentration of Hydrogen and for the loss increase at the 1 .24 µm. Hydrogen overtone as functions of time , for hydrogen pressure 1 atm and hydrogen loading temperature 21°C. Thus, for the 125 µm cladding diameter single-mode fiber, at 21°C, the molecular hydrogen losses will be within 95% of their equilibrium values in about 13 days, as the hydrogen approaches its equilibrium solubility of 116 ppm (where 1 ppm is defined as 10^{-6} moles of Hydrogen per mole of SiO_2). At higher temperatures, the equilibration is considerably faster. For instance, at 150°C the fiber will reach equilibrium in about 2 hours. From the test report of Paul J. Lemaire in Figure 2.16, There are four items which relate to this research. The first, hydrogen loss an proportional to hydrogen loading time. It mean, hydrogen loss is high when hydrogen loading time is long. The second, hydrogen loading temperature is high can accelerate hydrogen loss reach to saturated condition faster than the lower of hydrogen loading temperature. The last, hydrogen loss represent to hydrogen concentration.

2.1.7.3 Molecular-Hydrogen Diffusivity into the Fiber [9].

The molecular hydrogen penetrate phenomenon into the fiber optics which is expressed by a diffusion equation. Hence the time dependence of the loss increase due to molecular hydrogen is obtained by solving the diffusion equation. At a constant temperature, hydrogen concentration at the center of the fiber core exposed to hydrogen gas is expressed as equation (2.26)

$$C = C_{sat}\left[1 - \exp(-\lambda_i^2 D_H t / b^2)\right] \tag{2.26}$$

where C is the hydrogen concentration at the fiber-core center, C_{sat} is the saturated value of C, λ_i is the *i*th root which satisfies the zeroth order Bessel function $J_0(\lambda_i) = 0$, D_H, is diffusivity of hydrogen into silica, *t* is exposure time, and *b* is the fiber radius.

The temperature dependence of D_H is described by Arrhenius expression in the equation (2.27)

$$D_H = A \cdot \exp(-E_0 / RT) \tag{2.27}$$

where A is the frequency factor, R is the gas constant, T is the absolute temperature, and E_0 is the activation energy for the hydrogen diffusion into silica fiber. The Arrhenius plot for evaluated D_H is shown in Figure 2.19. The D_H values are closely fit for a straight line. The frequency factor and activation energy are evaluated from the fitting line and are 1.42 × cm^2/s and 10.8 kcal/mole, respectively.

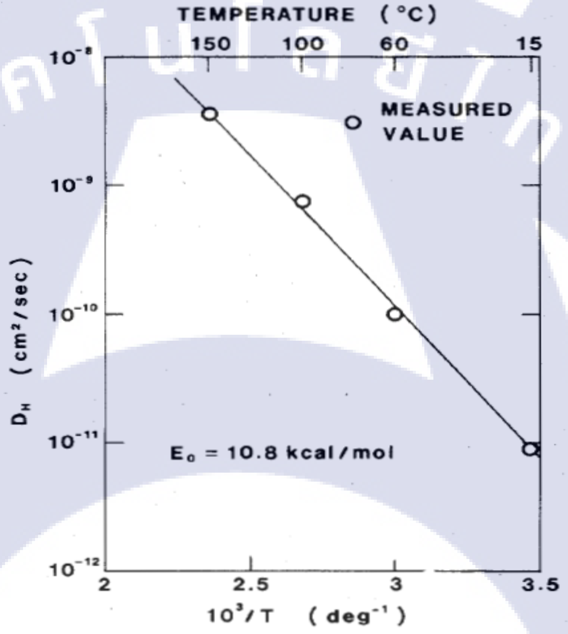

Figure 2.19 The evaluation for Diffusivity of fiber optics [9]

2.2 Literatures review

Y. Masuda et al perform two experiments to confirm FBG wavelength shift of hydrogen loading optics fiber during annealing process. There are two experiments which use to confirm wavelength shift of FBG during annealing process due to hydrogen gas out-diffusion. The first result compare the wavelength shift of FBG during annealing process at different annealing temperature with hydrogen diffusion theory. Wavelength shift pattern of LP-FBG was well consistent with hydrogen diffusion theory. The second result was comparison of FBG wavelength shift before and after Re-H_2 loading. The wavelength shift pattern of both conditions follow the same trend. Therefore, it was confirmed that FBG wavelength shift due to hydrogen out-diffusion [10]

P. L. Swart and A. A. Chtcherbakov perform experiments about hydrogen diffusion in Boron/Germanium codped optical Fiber. The result of their experiment reveal that no chemical interaction between hydrogen molecule and silica during hydrogen loading process. They measure hydrogen concentration from refractive index changem [11].

K. Noguchi et al. They studied loss increase for optical fibers exposed to hydrogen atmosphere. Optical-fiber loss-increase characteristics due to hydrogen were investigated from the loss spectrum change for the fibers exposed to hydrogen gas at the 15-200°C temperature range. Loss increase due to molecular hydrogen was investigated from the loss peak height, which appeared at the 1.24 μm wavelength in the loss spectrum. They found that physical solubility equation that the 3.4 dB/km loss increase at 1.24 μm is caused by 10l8 molecule/cm3 hydrogen permeation into optical fibers. The diffusivity of the hydrogen molecule into fibers which depend temperature and hydrogen pressure [9].

P. J. Lemaire studied research about reliability of optical fibers exposed to hydrogen: prediction of long-term loss increases. He reported that there are two kinds of loss mechanisms. Unreacted hydrogen loss and reacted hydrogen loss. Unreact hydrogen loss appear sharp peak at 1.24 μm from hydrogen molecule. On the other hand, reacted hydrogen loss that show peak around 1.4 μm from OH molecule. Hydrogen loss are function of temperature, time, and pressure [8].

T. Erdogan et al. Their research studied about Decay of ultraviolet-induced fiber bragg grating. The refractive index changing from UV radiation must decay by a “power law”. They propose a decay mechanism in which carriers excited during writing are trapped in a broad distribution of trap states, and the rate of thermal depopulation is an activated function of the trap depth. They also perform a decelerate-aging experiment. The result of the experiment found that to preanneal a grating can remove the portion of the index change that would decay over the lifetime of the grating [12].

Chapter 3

Research and methodology

This chapter is described the research methodology and technique identify hydrogen in fiber. There are three experiments in this chapter. The first experiment is to study the effect of hydrogen loading time at 48, 72, 120, and 192 hours to FBG parameter with sample size 10 pcs. The second experiment is to select the two candidate conditions from the first experiment. Then study the effect of these conditions with sample size 40 pcs. The last experiment is to select only one hydrogen loading condition for implementation with sample size 100 pcs. The research methodology flow is shown in Figure 3.1. The standard deviation of wavelength, reflectivity, bandwidth, and the average of writing time at writing process are considered as be the judgment factors for all of the experiment.

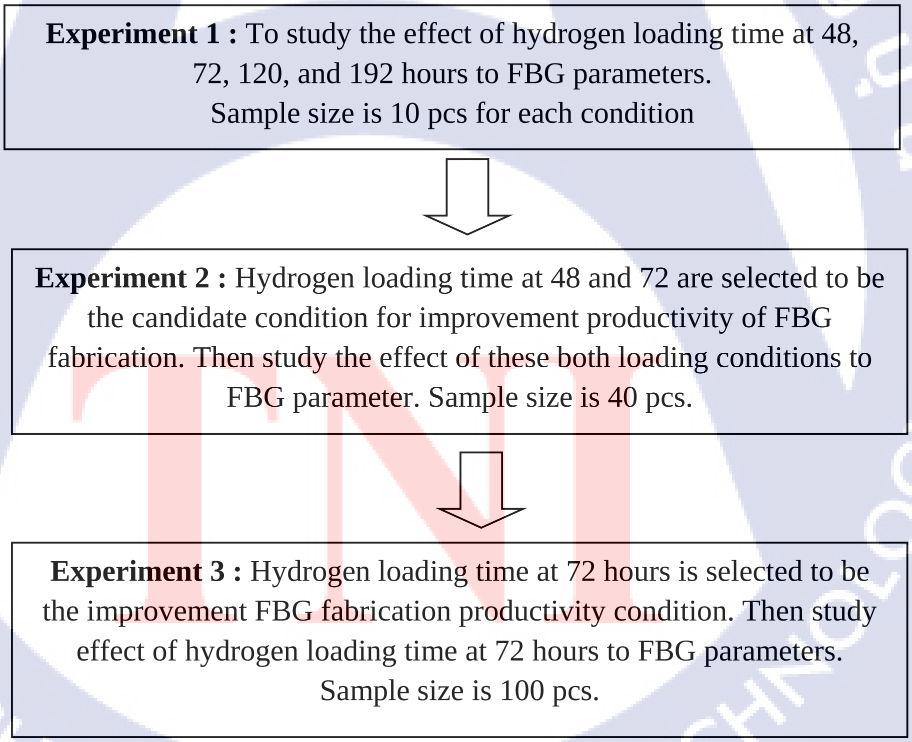

Experiment 1 : To study the effect of hydrogen loading time at 48, 72, 120, and 192 hours to FBG parameters. Sample size is 10 pcs for each condition

Experiment 2 : Hydrogen loading time at 48 and 72 are selected to be the candidate condition for improvement productivity of FBG fabrication. Then study the effect of these both loading conditions to FBG parameter. Sample size is 40 pcs.

Experiment 3 : Hydrogen loading time at 72 hours is selected to be the improvement FBG fabrication productivity condition. Then study effect of hydrogen loading time at 72 hours to FBG parameters. Sample size is 100 pcs.

Figure3.1 The research methodology flow

3.1 The overview of FBG fabrication process.

FBG fabrication process flow consists by these below processes as shown in Figure 3.2. The first process is hydrogen loading process then FBG is inscribed on fiber by writing process. To stabilize FBG area from high temperature at FBG thermal stabilization process. Then FBG is improved the strength by recoat process. Elimination hydrogen in fiber by heat from oven at hydrogen annealing process. Finally, evaluation FBG parameter at optical inspection process.

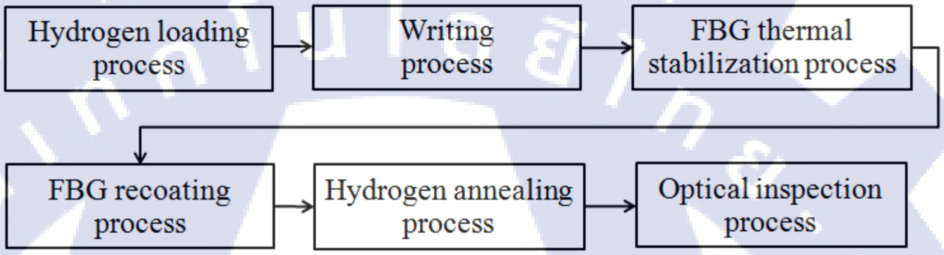

Figure 3.2 FBG fabrication process flow.

3.1.1 Hydrogen loading process.

The purpose of hydrogen loading process is to enhance photosensitivity of fiber. In this process, fiber bundles are put in the chamber as shown in Figure 3.3. Hydrogen gas is loaded in the system. The hydrogen loading temperature depends on environment temperature due to the chamber room is an open system.

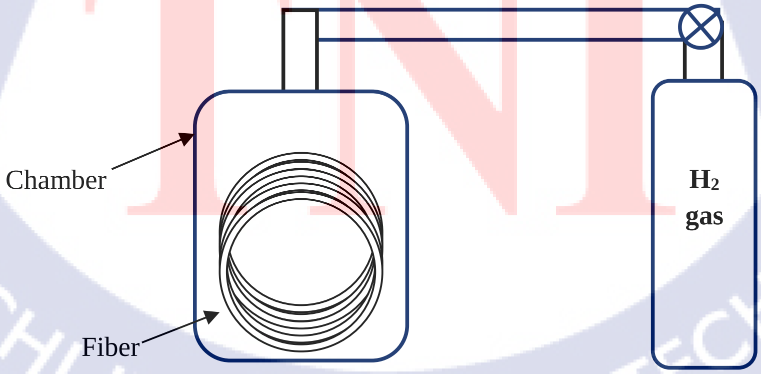

Figure 3.3 A schematic of hydrogen loading process

3.1.2 Writing process.

The objective of writing process is to inscribe FBG on fiber. There are several techniques inscribe FBG. In this research implement UV light with phase mask technique to change the refractive index of fiber core. Before FBG will be exposed to UV light, fiber has to be removed coating polymer for glass area preparation. The example of FBG inscribing by phase mask technique is demonstrated in Figure 3.4.

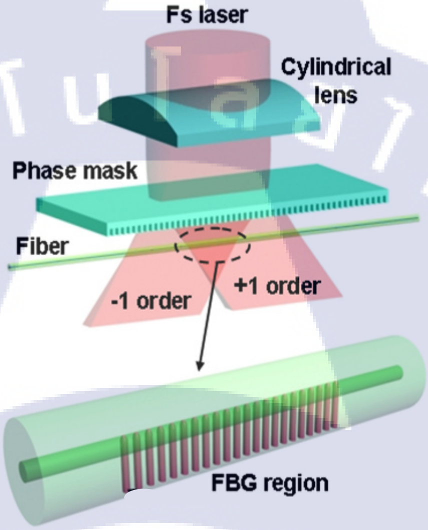

Figure3.4 A schematic of phase mask technique to inscribe FBG on fiber at writing process.

3.1.3 FBG thermal stabilization process.

The objective of FBG thermal stabilization process is to stabilize FBG parameter in long term by applying high temperature to FBG area. The FBG stabilization by heat as shown in Figure 3.5.

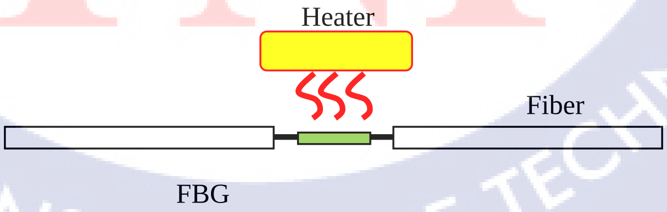

Figure 3.5 To stabilize FBG by high temperature at FBG thermal stabilization process

3.1.4 Recoat process.

FBG area is the fiber that remove coating polymer. Therefore, FBG area is a glass, glass is sensitive to damage. To improve the strength of FBG, adhesive UV-resin is coated on FBG area. This process is called recoat process. The UV resin is coated on FBG area as shown in Figure 3.6.

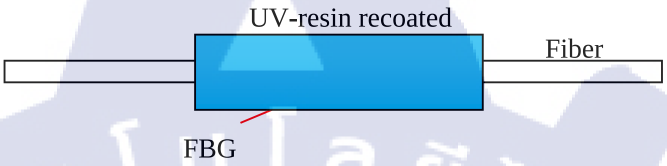

Figure3.6 UV resin is coated on FBG area at Recoat process.

3.1.5 Hydrogen annealing process.

To eliminate hydrogen from fiber, we input fiber in the oven that is called hydrogen annealing process. The heat from oven accelerate hydrogen molecule diffuse from fiber. Hydrogen is needed to eliminate from fiber due to FBG wavelength shift to shorter wavelength when hydrogen diffuse from fiber. This phenomenon is explained in chapter2.

3.1.6 Optical inspection process.

Finally, To evaluate FBG parameters including FBG wavelength, eflectivity, and bandwidth with the spec before shipping at optical inspection process.

3.2 The research methodology plan

In this research including by three experiments. The explanation of each experiment is as follow items.

3.2.1 Experiment 1: To study effect of hydrogen loading time at 48, 72, 120, and 192 hours to FBG parameters. Sample size is 10 pcs for each condition.

In this experiment, Single mode fiber are loaded hydrogen at 13 MPa. Hydrogen loading time were varied at 48, 72, 120, and 120 hours. After finishing from hydrogen loading process, fiber are storage in the freezer at low temperature.

The low temperature prevents hydrogen diffuse from fiber. At writing process, UV laser and phase mask technique are used for inscribe FBG. Laser power, phase mask pitch, reflectivity target are controlled for all testing conditions.

After writing process, all of FBG is stabilized at high temperature. Then improve the FBG strength by UV-resin coating. Elimination all of hydrogen in fiber by input them in oven. Finally, measure FBG parameter at optical inspection process.

3.2.2 Hydrogen loading time at 48 and 72 are selected to be the candidate condition for hydrogen loading process. Then study the effect of these both loading conditions to FBG parameter. Sample size is 40 pcs.

From the result of the first experiment, hydrogen loading time at 48 and 72 hours are the candidate. In this experiment, both hydrogen loading time conditions are selected to study the effect of hydrogen loading time to FBG parameter with sample size 40 pcs.

Single mode fiber was loaded hydrogen gas at pressure 13 MPa. Hydrogen loading time are varied at 48 and 72 hours. The other processes flow are similar as the first experiment.

3.2.3 Experiment 3: Hydrogen loading time 72 hours is selected to be the best condition. Then study the effect of hydrogen loading time at 72 hours to FBG parameters with sample size 100 pcs.

The result of the second experiment reveals that hydrogen loading time 72 hour is better than 48 hours. Therefore, hydrogen loading time at 72 hours is selected to study the effect of hydrogen loading time to FBG parameters with Polarization maintaining fiber (PMF). Due to there are various type of fiber in FBG manufacturing for this reason, it is needed to study the effect of hydrogen to fiber type.

PMF fiber is loaded hydrogen gas at pressure 13 MPa. Hydrogen loading time is controlled at 72 hours. The process flow of this experiment is similar to the previous experiment. The reflectivity target of this test at writing process is less than the previous experiment around 50%. The summarize information of each experiment as shown in Table 3.1.

Table 3.1 The summarize information of each experiment

Experiment	Sample size (pcs.)	H_2 pressure (MPa.)	H_2 loading time (Hours.)	Reflectivity (%)	FBG wavelength (nm.)	Fiber type
1	10	13	48,72, 120, and 192	4	980	SMF
2	40	13	48 and 72	4	980	SMF
3	100	13	72	1	1480	PMF

Where H_2 is Hydrogen gas, SMF and PMF are Single mode fiber and Polarization maintaining fiber respectively. Reflectivity target and FBG wavelength belong to optical inspection process

3.3 Hydrogen absorption loss technique.

Hydrogen absorption loss is used to evaluate the amount of hydrogen molecule in fiber. This technique can install the measurement system as shown in Figure 3.7. We use the optical light source at wavelength range over than 1000 nm to measurement hydrogen loss. Due to the transmission loss spectrum of hydrogen shows at wavelength range around 1240 nm. The Optical spectrum analyzer (OSA) is an instrument to measure and display the distribution of power of an optical source over a specified wavelength span. OSA parameter setting as shows in Table 3.2.

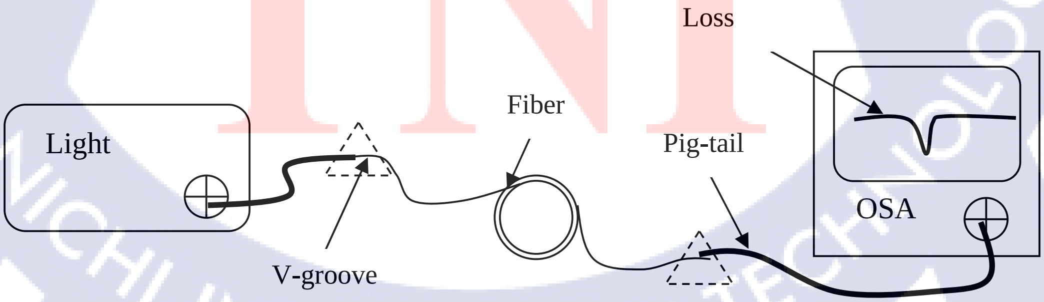

Figure 3.7 A schematic of hydrogen loss measurement installation

Table 3.2 Optical spectrum analyzer setting parameter to measure hydrogen absorption loss

Optical spectrum analyzer parameters	**Setting value**
Start wavelength(nm)	1200
Stop wavelength(nm)	1300
Span(nm)	100
Resolution(nm)	1
Sampling rate	501

3.3.1 The method for calculation hydrogen loss

Hydrogen absorption loss is obtained by the different between the maximum and minimum point from transmission spectrum as show in Figure 3.8.

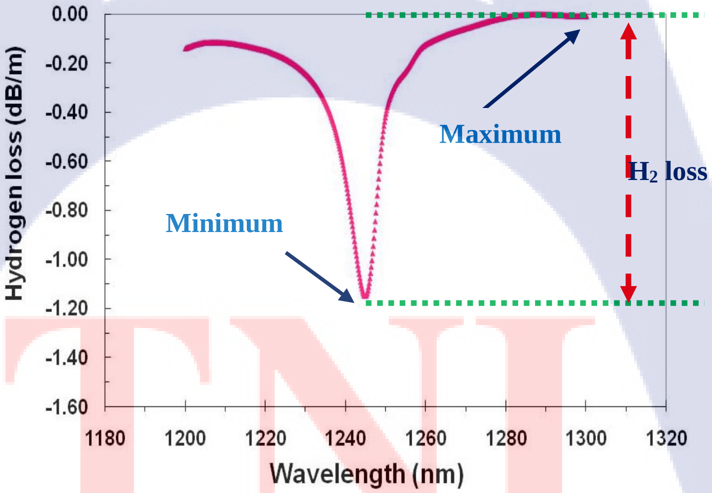

Figure 3.8 Hydrogen loss is obtained from the different of hydrogen loss between the maximum and minimum point from transmission spectrum.

Chapter 4

Experimental results and Discussions

This chapter is presented the results and discussion of the experiment. In this research consist of three experiment results. The point of the first experiment result is to study the effect of hydrogen loading time to FBG parameters and evaluation of hydrogen concentration in fiber of each hydrogen loading condition. The objective of the second experiment result is to verify the first experiment result with increasing of the sample size. The final experiment result is explained the effect of the best hydrogen loading condition which can improve productivity of FBG fabrication.

4.1 Experiment 1 : To study the effect of hydrogen loading time at 48, 72, 120, and 192 hours to FBG parameters. Sample size is 10 pcs for each condition.

4.1.1 Evaluation hydrogen concentration in fiber in term of hydrogen loss.

Before discussing the effect of hydrogen loading time to FBG parameters. The evaluation of hydrogen concentration in fiber at the various of hydrogen loading time are necessary to be studied. The experiment installation of this experiment was shown in Figure3.6. The result of this experiment was shown by transmission spectrum of light at wavelength range around 1240 nm as shown in Figure4.1.

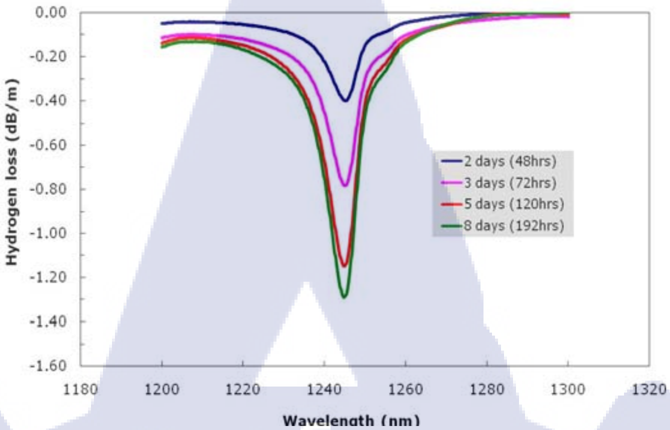

Figure 4.1 Hydrogen absorption loss peak at 1240 nm at hydrogen loading time 48,72,120, and 192 Hours.

From transmission spectrums in Figure4.1, all of hydrogen loading conditions shown sharp peak at wavelength around 1240 nm. The peak that shown on this wavelength was indicated to the hydrogen molecule in fiber. Hydrogen loss calculation from transmission spectrum reveal that hydrogen loss is high when hydrogen loading time is long as shown in Table4.1.

Table4.1 The hydrogen loss from the experiment of hydrogen loading time at 48, 72, 120, and 192 hours.

Hydrogen loading time(Hrs.)	Hydrogen loss (dB/m.)
48	0.37
72	0.72
120	1.09
192	1.21

In this research, the relation of hydrogen concentration in fiber with hydrogen loading time was expressed as [9].

$$C = C_{sat}\left[1 - \exp(-\lambda_i^2 D_H t / b^2)\right] \tag{4.1}$$

Where C is the hydrogen concentration at the fiber-core center. C_{sat} is the saturated value of C. λ is the *i*th root, which depends on the zeroth order Bessel function, D_H is diffusivity of hydrogen into silica, t is hydrogen loading time, and b is the fiber radius.

Kazuhiro and teams were used Multi mode fiber that core size 50 μm and cladding size 125 μm to be material for hydrogen loading process. They used equation (4.1) to verify the relation of hydrogen loading time to hydrogen concentration in fiber. In our research, Single mode fiber which core size 5-9 μm and cladding size 125 μm were loaded hydrogen gas. Core and cladding size of single and multi mode fiber was shown in Figure4.2.

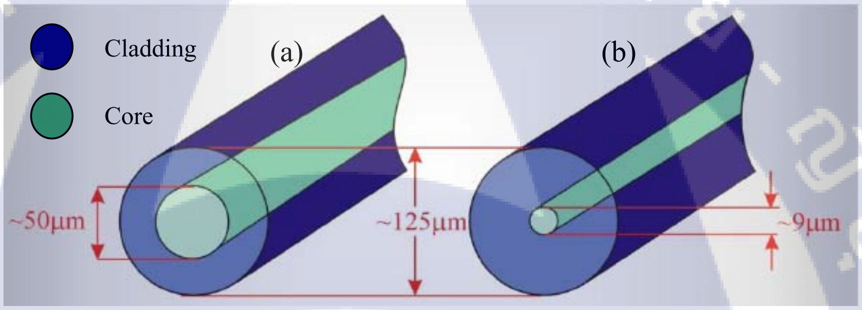

Figure 4.2 Core and cladding size diameter (a.) Common of fiber structure, (b.) Core and cladding size of single mode fiber, (c.) Core and cladding size of multi mode fiber [13].

To reach the similar of hydrogen concentration in fiber, multi mode fiber spend hydrogen loading time shorter than single mode fiber. Due to the distance between core and cladding is shorter than single mode fiber. This affect to hydrogen gas penetrate through the coating layer of fiber rapidly. The second layer is cladding which commonly make from glass. The penetration rate of hydrogen gas from cladding to fiber core is lower than hydrogen gas penetrate from outside to coating layer of fiber. Therefore, the different size of fiber core, it lead to the different of hydrogen concentration in fiber core at the same of hydrogen loading time as shown in Figure 4.3.

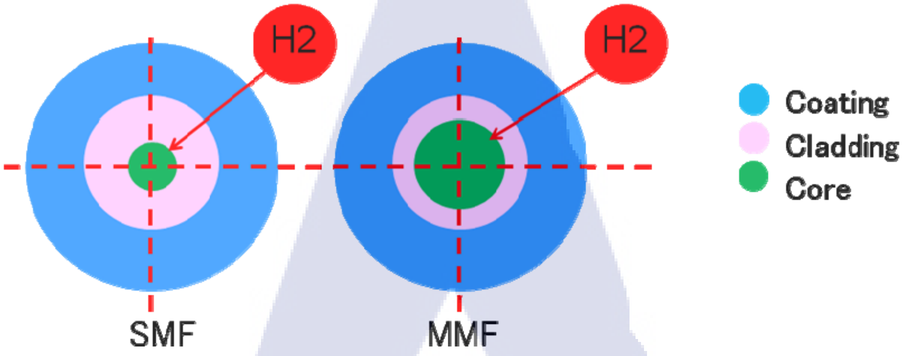

Figure 4.3 Core and cladding size diameter (a.) Common of fiber structure, (b.) Core and cladding size of single mode fiber, (c.) Core and cladding size of multi mode fiber.

In this research, we apply the equation 4.1 to appropriate with our fiber type as shown in equation 4.2

$$L = L_{sat}\left[1-\exp(-\lambda_i^2 D_H (t - t_{cladding})/b^2)\right] \quad \text{for} \quad t>24 \quad \text{Hrs.} \tag{4.2}$$

Where L is the hydrogen loss at the fiber-core center. L_{sat} is the saturated value of L. λ is the *i*th root, which depends on the zeroth order Bessel function, D_H is diffusivity of hydrogen into silica, t is hydrogen loading that hydrogen molecule penetrate to cladding area, $t_{cladding}$ is hydrogen loading time that hydrogen molecule penetrate to core area, and b is the fiber radius. Hydrogen loss is a function of hydrogen concentration. Therefore, in this research, hydrogen loss was represented to hydrogen concentration. The effect of core size of fiber, $t_{cladding}$ is add to equation(4.2) to present that single mode fiber need to include time for hydrogen penetration from cladding to core area. In this research, $t_{cladding}$ is 24 Hrs. This value came from the extrapolation of experiment data. L_{sat} is hydrogen loss at saturated value. Hydrogen loss 1.3 dB/m to be a hydrogen loss at saturation value in the equation.

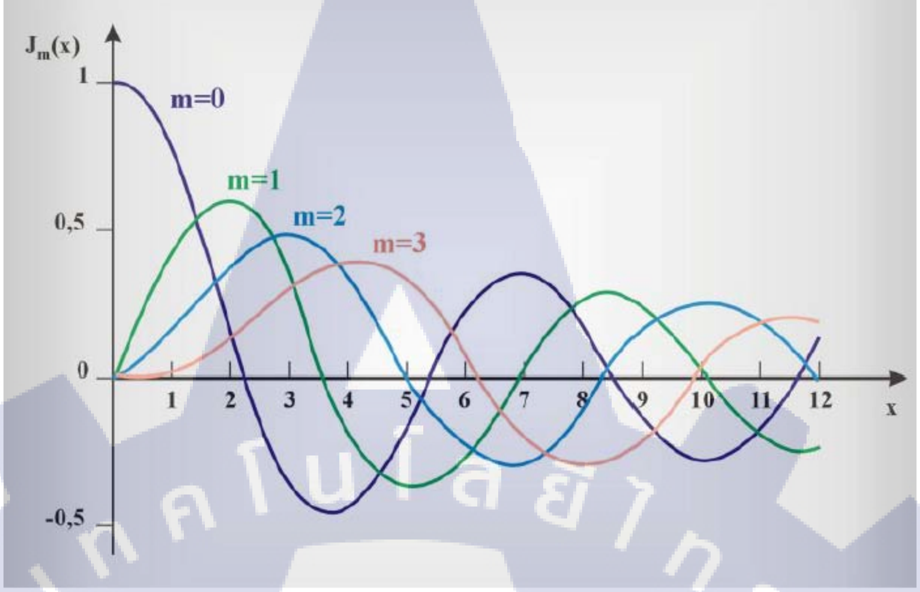

Figure 4.4 The Bessel functions of the first kind $J_n^{(X)}$ are defined as the solutions to the Bessel differential equation [3].

λ is *i*th root, which depends on the zeroth order Bessel function. λ is 2.3 that came from Figure4.4. D_H is diffusivity of hydrogen into silica (cm^2/sec.) which obtain from equation (4.3) [9].

$$D_H = A \cdot \exp(-E_0 / RT) \qquad (4.3)$$

Where A is the frequency factor(cm2/sec), *E₀* is The activation energy (kcal/mole), R is a gas constant (cal/mol.K), and T is hydrogen loading temperature (K). In the hydrogen loading process, hydrogen loading time was 308 K. The R is 1.99 cal/mol.K. The factors A and *E₀* are $1.42 \times 10^{-3} cm^2 / \sec$ and 10.8 kcal/mole respectively. After apply these factors value in equation (4.3). D_H is expressed by equation (4.4)

$$D_H = 1.42 \times 10^{-3} \cdot \exp(\frac{-10.8 kcal / mole}{RT}) cm^2 \sec^{-1} \qquad (4.4)$$

b is a fiber radious, cladding diameter of single mode fiber is 125 µm.

Therefore, b is 62.5 µm. The factor $t_{cladding}$ is 20 hours. This mean, if hydrogen loading time less than 24 hours. The hydrogen concentration in fiber core is zero.

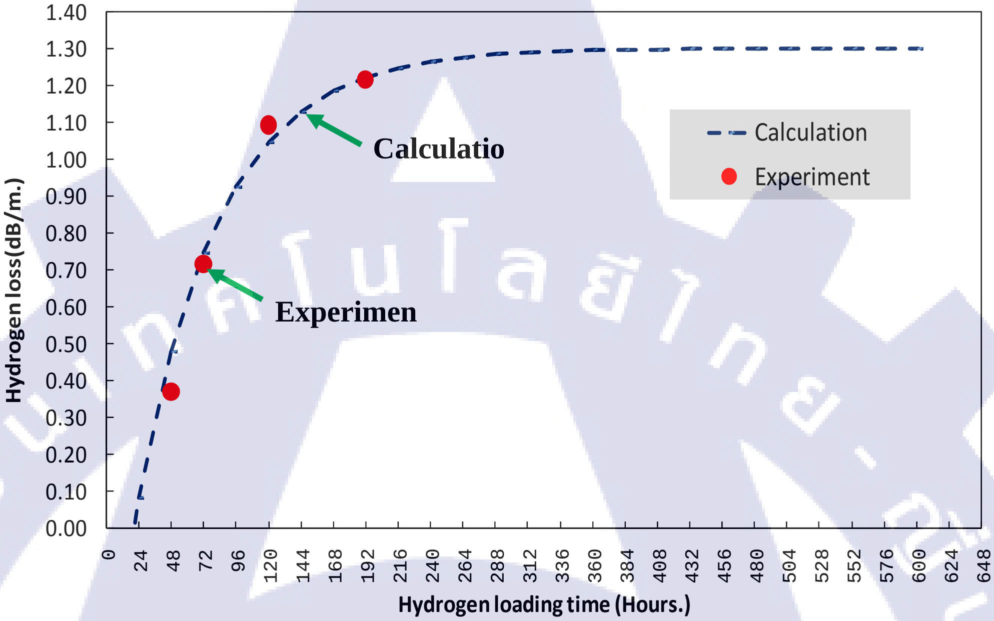

Figure 4.5 The verification result of hydrogen loss from the experiment and hydrogen loss from equation (4.2).

Figure4.5 showed the measurement hydrogen loss from the experiment that represent by red dot. The dash line refers to hydrogen loss obtained from equation (4.2). The experiment data was consistent to the calculation data. Therefore, hydrogen concentration is a proportional to hydrogen loading time, hydrogen concentration at saturated value of this experiment should be 336 hours.

4.1.2 The effect of hydrogen loading time to FBG parameter.

The important parameters of FBG consist of four parameters. In this chapter, the effect of hydrogen loading time to FBG wavelength, reflectivity and bandwidth are reported.

4.1.2.1 The effect of hydrogen loading time to writing time.

The purpose of hydrogen loading process is to enhance photosensitivity of fiber. Photosensitivity reveal in term of writing time at writing process. Therefore, writing time is the first priority to evaluate when hydrogen loading time is changed.

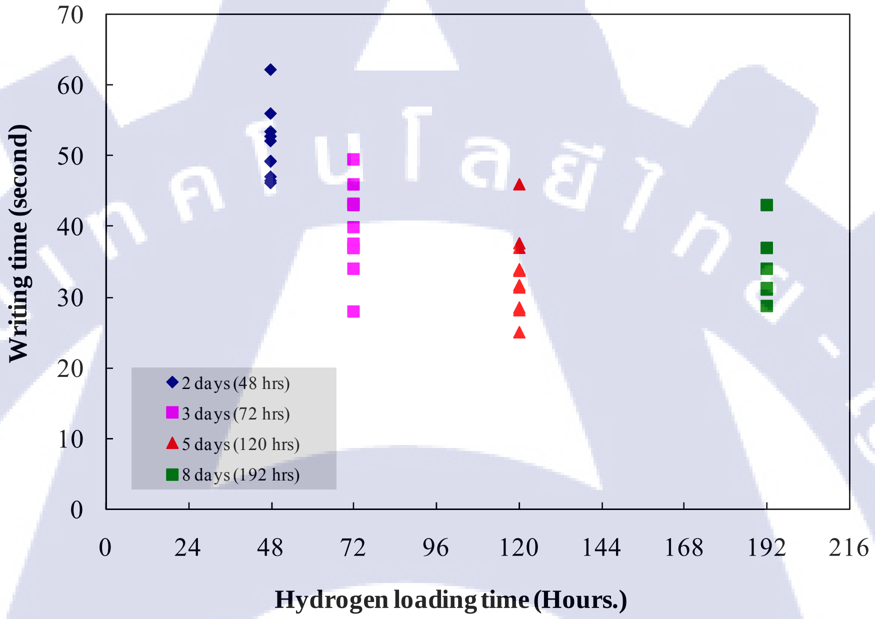

Figure 4.6 The distribution of writing time at hydrogen loading time 48, 72,120, and 192 Hours.

Figure4.6 shown the distribution of writing time for hydrogen loading time at 48, 72, 120, and 192 hours. The writing time is short when hydrogen loading time is long. This came from photosensitivity effect. According to the experiment result from Figure4.5, it was revealed that hydrogen concentration is high when hydrogen loading time is long. Due to GODC is reacting with UV light also high. This lead to high of photosensitivity during writing process. To improve FBG productivity, the cycle time at hydrogen loading process was reduce on the other hand the cycle time at writing process was increased from the low of hydrogen concentration in fiber. However, the writing time of the shortest of hydrogen loading time is still under control limit of FBG manufacturing therefore, all of hydrogen loading conditions were accepted.

4.1.2.2 The effect of hydrogen loading time to FBG wavelength

In chaper2 on section of literatures review, Yuji Masuda and team were described the effect of hydrogen to FBG wavelength shift. The FBG wavelength shift quantity can imply the hydrogen concentration in fiber. The side effect of hydrogen molecule penetrate in fiber is to increase refractive index of fiber core. This affect to FBG wavelength shift to shorter wavelength when hydrogen molecules diffuse from FBG. The definition of FBG wavelength is expressed by equation (4.5).

$$\lambda_b = 2n_{eff}\Lambda \tag{4.5}$$

Where λ_b is Bragg wavelength, n_{eff} is effective index , and Λ is grating pitch, phase mask technique was used to inscribe FBG therefore the relation of grating pitch to phase mask pitch is $\Lambda_{grating} = (\frac{\Lambda_{phasemask}}{2})$, the relation of n_{eff} to refractive index change by hydrogen molecule is expressed by equation (4.6).

$$n_{eff} = average(n_{fibercore} + n_{hydrogen} + n_{UVinduce}) \tag{4.6}$$

Where $n_{fibercore}$ is the original refractive index of fiber core, $n_{hydrogen}$ is refractive index change from hydrogen molecule penetrate in fiber core, and $n_{UVinduce}$ is refractive index of fiber core changing from UV photo induce refractive index change.

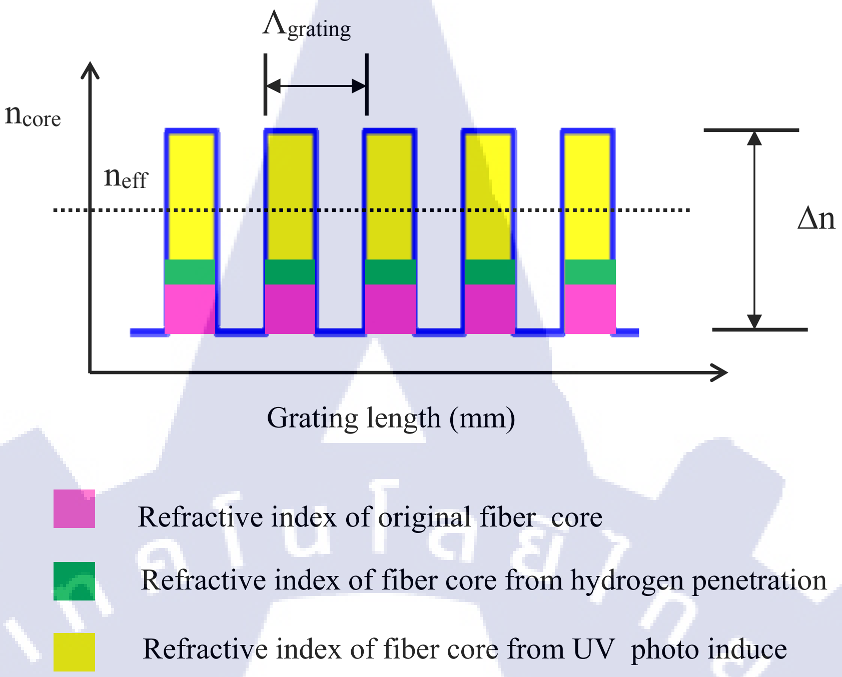

Figure 4.7 The schematic of refractive index of FBG changing.

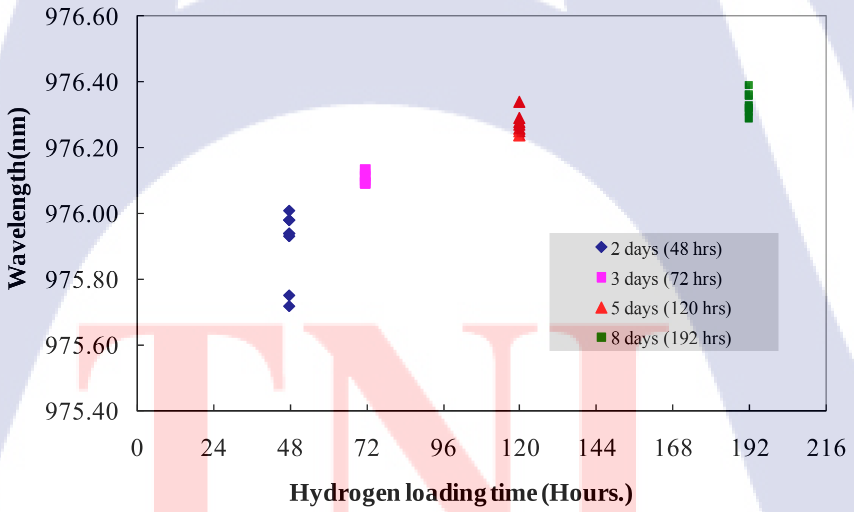

Figure 4.8 The distribution of FBG wavelength at writing process for hydrogen loading time at 48,72,120, and 192 Hours.

The result of FBG wavelength at writing process was shown in Figure4.8. It can be seen that FBG wavelength was long when hydrogen loading time was long.

The FBG wavelength distribution result was explained by the relation of refractive index of fiber core with FBG wavelength as shown in equation (4.5) and (4.6). In this experiment, the phase mask pitch number at writing process was controlled for all conditions. Therefore, FBG wavelength was long when hydrogen loading time was long affect from the refractive index of fiber core increasing from hydrogen loading ($n_{hydrogen}$). Therefore the summation of effective index (n_{eff}) was increased when hydrogen loading time was long. In contrast, FBG wavelength became similar for all condition at optical inspection process. The experiment result of FBG wavelength at optical inspection process was shown in Figure4.9.

According to FBG process flow in Figure 3.2 at chapter3. There was two processes that generate heat to FBG area.

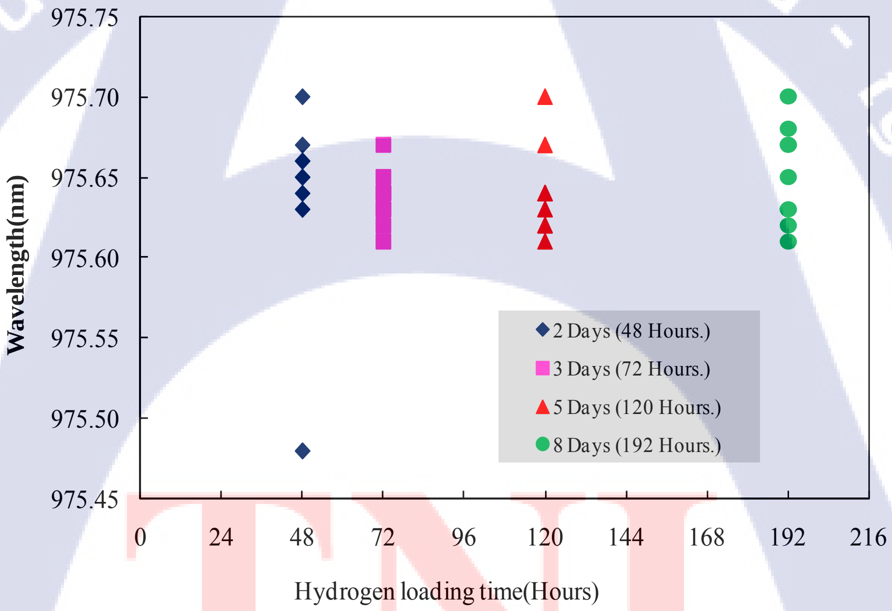

Figure 4.9 The distribution of FBG wavelength at optical inspection for hydrogen loading time at 48,72,120, and 192 Hours.

The heat from these two processes accelerated hydrogen molecule diffused from fiber core. Therefore, the effective index of fiber core reduction (n_{eff}) from the elimination of hydrogen ($n_{hydrogen}$) and unstable portion of refractive index change.

For judgment of FBG wavelength at different of hydrogen loading time, the standard deviation of FBG wavelength at optical inspection process at condition 72, 120, and 192 hours were accepted. In case of 42 hours, the standard deviation of FBG wavelength at optical inspection process was 0.08 nm. This value was higher than other condition as shown in Table4.2. The fluctuation of FBG wavelength of condition 42 hours, it might affect from some effect during FBG writing at writing process. It might not affect from hydrogen loading time. However, to verify the fluctuation of FBG wavelength at 42 hours. The sample should be increased.

Table4.2 The standard deviation of FBG wavelength at optical inspection process

Hydrogen loading time(Hrs.)	Standard deviation (nm.)	Specification of Standard deviation of FBG wavelength (nm.)	Judgment
48	0.08	0.12-0.15	Accept
72	0.02		Accept
120	0.03		Accept
192	0.03		Accept

4.1.2.3 The effect of hydrogen loading time to FBG reflectivity

Reflectivity is an important parameter of FBG. The definition of reflectivity is expressed by equation (4.7).

$$\left|\rho\right|^2 = \tanh^2(KL) \tag{4.7}$$

Where $\left|\rho\right|^2$ is reflectivity, K is coupling coefficient, and L is grating length. K is defined by equation (4.8).

$$K = \frac{4\prod \eta \Delta n}{\lambda_b} \tag{4.8}$$

Where η is an Eta, Δn is refractive index change as shown in Figure4.7, and λ_b is Bragg wavelength.

Figure4.10 was shown the distribution of reflectivity at writing process of hydrogen loading time at 48, 72, 120, and 192 hours.

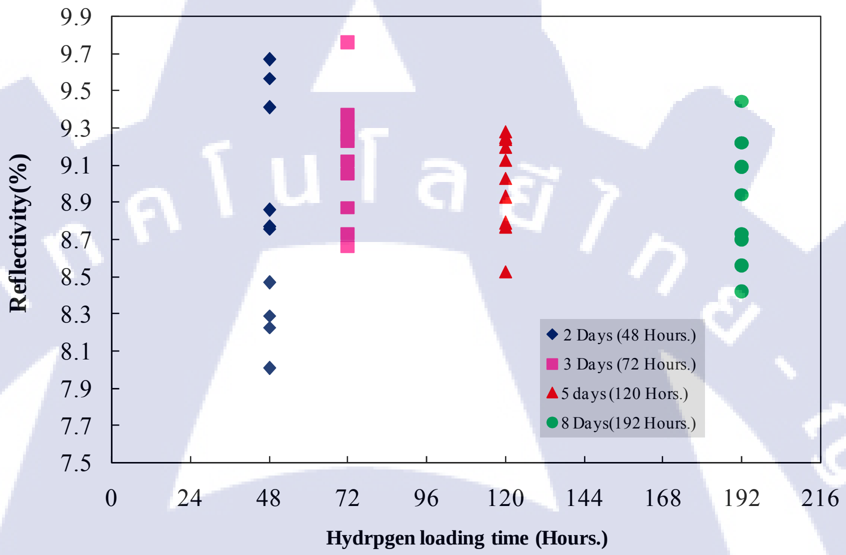

Figure 4.10 The distribution of FBG reflectivity at writing process for hydrogen loading time at 48,72,120, and 192 Hours.

Table4.3 The standard deviation of FBG wavelength at optical inspection process

Hydrogen loading time(Hrs.)	**Standard deviation (%)**	**Specification of Standard deviation of FBG reflectivity (%)**	**Judgment**
48	0.17	0.16-0.20	Accept
72	0.29		Not Accept
120	0.13		Accept
192	0.06		Accept

From equation (4.7) and (4.8), the relation of hydrogen to reflectivity were shown in factor of Δn and λ_b. At writing process, reflectivity target was controlled to be same for all conditions, therefore Δn of shortest hydrogen loading time should be higher other condition. In case of λ_b, hydrogen loading time was long affect to FBG wavelength at writing was long. λ_b is reverse function to reflectivity. This leaded to reflectivity at writing process should be low when hydrogen loading time was long. The result from experiment was shown in Figure4.10 consistent to the theory of reflectivity as expressed in equation (4.7) and (4.8). However, the difference of reflectivity of all hydrogen loading condition was slightly different. This effect came from the low of refractive index change by hydrogen loading ($n_{hydrogen}$) when it was compared to refractive index change (Δn). In case the distribution of reflectivity result at optical inspection process as shown in Figure 4.11.

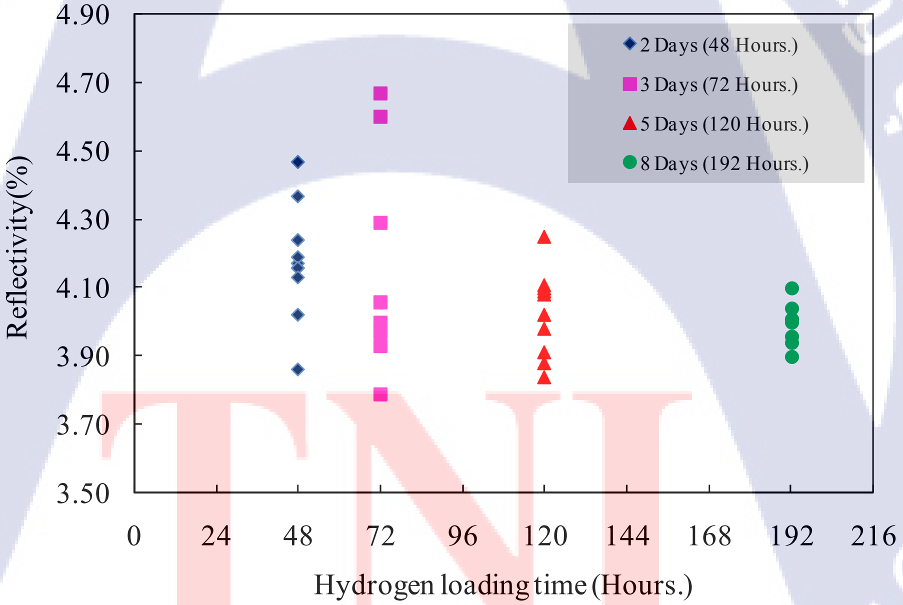

Figure 4.11 The distribution of FBG reflectivity at optical inspection process for hydrogen loading time 48,72,120, and 192 Hours.

It can be seen in Figure 4.11 that the FBG reflectivity at optical inspection process were reduced from reflectivity at writing process. This affect from heat at

FBG thermal stabilization and hydrogen annealing processes. Heat from these processes eliminated the refractive index change (Δn) .And refractive index change from hydrogen ($n_{hydrogen}$). Therefore, the final refractive index of fiber core was reduced when compare with reflective index at writing process. The standard deviation of reflectivity were similar in case of 42, 120, and 192 hours and it was under FBG fabrication control level. The standard deviation of reflectivity at 72 hours was higher than other conditions as shown in Table4.3. This fluctuation of reflectivity might not affect from hydrogen loading time due to the effect of hydrogen loading time to reflectivity should be revealed at writing process. Although, the distribution of reflectivity at 72 hours of writing process was less than 42 hours. It was shown in Figure 4.11. Therefore, the fluctuation of reflectivity at 72 hours might fluctuate from the process that eliminates refractive index of fiber core.

4.1.2.4 The effect of hydrogen loading time to FBG bandwidth.

Bandwidth is an important parameter of FBG. The definition of FBG bandwidth is expressed by equation (4.9).

$$\Delta\lambda = \frac{\lambda_b^{\ 2}}{2\prod n_{eff} L}\sqrt{(KL)^2 + \prod^2} \qquad (4.9)$$

Where $\Delta\lambda$ is bandwidth from the peak to the first Zero, λ_b is Bragg wavelength, n_{eff} is effective index, K is coupling coefficient, and L is grating length. From equation (4.9), The effect of hydrogen loading time to bandwidth should be show in term of λ_b and n_{eff}. These factors were divided to each other and they were equality in term of refractive index. Therefore, hydrogen loading time unaffected to FBG bandwidth. The experiment result of bandwidth at writing process of hydrogen loading time at 48, 72, 120, and 192 hours were shown in Figure4.12.

From the experiment result in Figure4.12, there are on trend of bandwidth when hydrogen loading time was changed. To verify the unaffected of hydrogen loading time to bandwidth. It can verify unaffected of hydrogen loading time to bandwidth from distribution of bandwidth at optical inspection process. That was shown in Figure 4.13

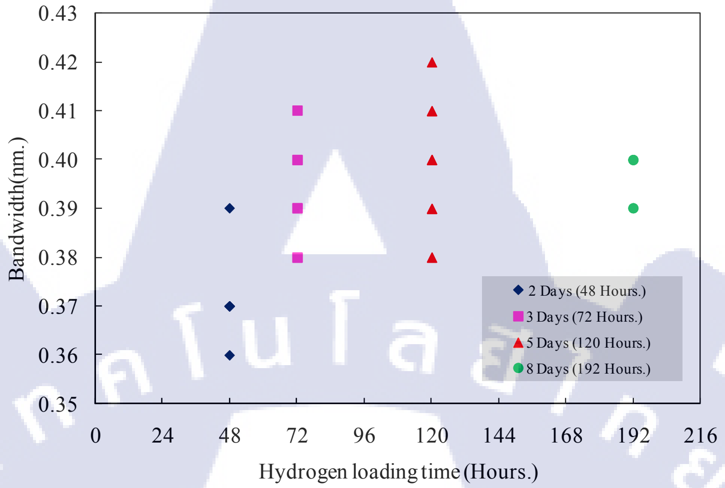

Figure 4.12 The distribution of FBG bandwidth at writing process for hydrogen loading time at 48,72,120, and 192 Hours

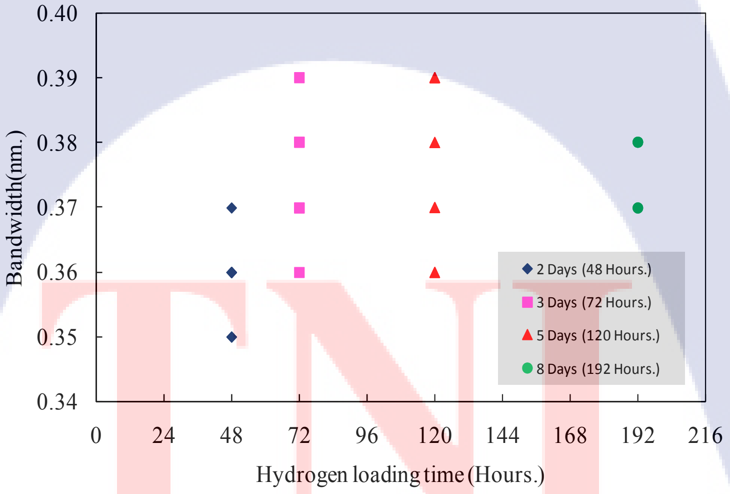

Figure 4.13 The distribution of FBG bandwidth at optical inspection process for hydrogen loading time at 48,72,120, and 192 Hours.

FBG bandwidth of hydrogen loading time at 48, 72, 120, and 192 hours at optical inspection process were less than bandwidth at writing process around 0.01-

0.02 nm. This revealed that hydrogen loading time unaffected to bandwidth. If hydrogen loading time affect to bandwidth, the bandwidth value might reduce when hydrogen was eliminated. The main factor that high impact to FBG bandwidth is grating length (L). From equation (4.9), bandwidth size is an inverse function of grating length(L). In this test, the grating length were controlled by UV beam size for all condition at writing process.

Table4.4 The standard deviation of FBG bandwidth at optical inspection process

Hydrogen loading time(Hrs.)	**Standard deviation (nm.)**	**Specification of Standard deviation of FBG bandwidth (nm.)**	**Judgment**
48	0.01	0.014-0.018	Accept
72	0.01		Accept
120	0.01		Accept
192	0.01		Accept

4.1.3 Conclusions

The different of hydrogen loading time mainly affect to writing time at writing process, FBG wavelength, and FBG reflectivity. However, the average of writing time of all hydrogen loading time conditions was accepted. In case of FBG wavelength, reflectivity, and bandwidth, standard deviation was considered to be the judgment factor. The standard deviation of wavelength at 48 hour and reflectivity at 72 hours were higher than other conditions. These fluctuation might not affect from hydrogen loading time. However, to verify this assumption, the experiment two were study effect of hydrogen loading time at 48 and 72 hours with sample size 40 pcs.

4.2 Experiment 2 : Hydrogen loading time 48 and 72 were selected to evaluate the effect of hydrogen loading time to FBG parameter with sample size 40 pcs.

After we understood the effect of hydrogen loading time to FBG parameter from the first experiment. We found that hydrogen loading time 48 and 72 hours should be the competitive conditions for improve FBG productivity fabrication as well as, sustain a quality of FBG. However, we would like to verify the fluctuation of FBG wavelength and reflectivity of hydrogen loading time 48 and 72 respectively by increasing the sample size from 10 pcs to 40 pcs.

4.2.1 The effect of hydrogen loading time to FBG wavelength.

The result from this experiment was used for verifying the fluctuation of FBG wavelength at optical inspection process of hydrogen loading time at 48 hours in the first experiment. Figure4.14 was shown histogram of FBG wavelength at optical inspection process for hydrogen loading time 48 and 72 hours. The FBG wavelength distributions of both conditions were similar. This result can verify the fluctuation of FBG wavelength at 48 hours from the first experiment did not effect from hydrogen loading time

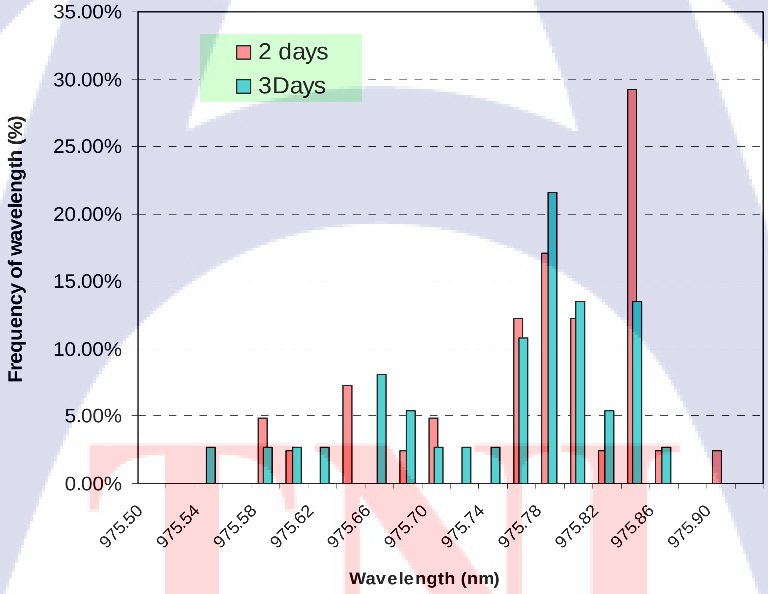

Figure 4.14 Histogram of FBG wavelength at optical inspection process for hydrogen loading time 48 and 72 Hours.

Table 4.5 Statistical data of FBG wavelength at different of hydrogen loading time of experiment

Hydrogen loading time(Hrs.)	**Standard deviation (nm.)**	**Specification of Standard deviation of FBG wavelength (nm.)**	**Judgment**
48	0.080	0.12-0.15	Accept
72	0.081		Accept

4.2.2 The effect of hydrogen loading time to FBG reflectivity at optical inspection process.

The result from this experiment was used for verifying the fluctuation of reflectivity at optical inspection process of hydrogen loading time at 72 hours in the first experiment. Figure 4.15 shown histogram of FBG reflectivity of both hydrogen loading conditions. The distribution of both hydrogen loading condition were similar. Therefore, the difference of hydrogen loading time did not affect to the fluctuation of FBG reflectivity.

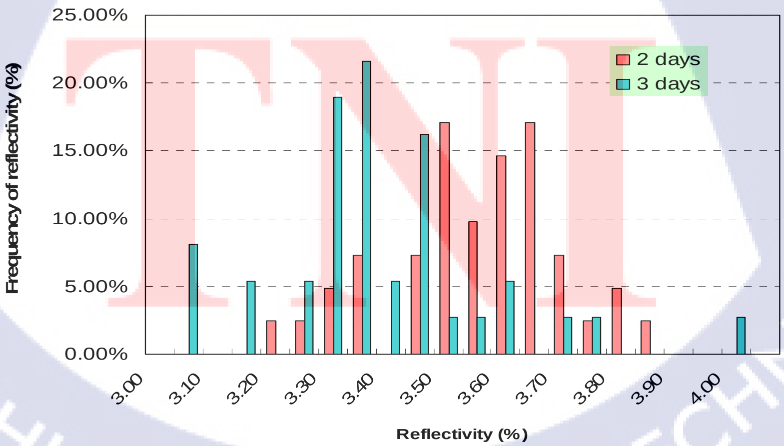

Figure 4.15 Histogram of FBG reflectivity at optical inspection process for hydrogen loading time 48 and 72 Hours.

Table 4.6 Statistical data of FBG reflectivity(%) at different of hydrogen loading time for experiment 1

Hydrogen loading time(Hrs.)	Standard deviation (%)	Specification of Standard deviation of FBG reflectivity (%)	Judgment
48	0.150	0.16-0.20	Accept
72	0.190		Accept

From Table 4.5 and 4.6, the standard deviation of all FBG parameter of both hydrogen loading conditions were similar and these value was under FBG production control limit. However, in case of the average writing time and the fluctuation of writing time, hydrogen loading time at 72 hours was better than 48 hours. Therefore, to improve hydrogen loading time as sustain the quality of FBG, hydrogen loading time at 72 hours was selected.

4.2.3 Conclusion

The fluctuation of FBG wavelength and reflectivity of hydrogen loading time 48 and 72 hours from the first experiment did not effect from hydrogen loading time. Hydrogen loading time at 72 hours was better than 48 hours in case of the shorter of writing time and the low fluctuation of writing time.

There are several type of fiber in FBG manufacturing. It is important to study the effect of hydrogen loading time to another type of fiber. The objective of the last experiment is to study the effect of hydrogen loading time 72 hours to PMF fiber.

4.3 Experiment 3 : To study the effect of hydrogen loading time 72 hours to FBG parameters with PMF fiber at sample size 100 pcs.

There are several types of fiber in FBG manufacturing. The different type of fiber provides the difference of fiber structure. From the experiment result section 4.1.1, the different size of cladding and core fiber affect to hydrogen concentration in fiber. Therefore, the effect of hydrogen loading time to PMF fiber was studied in this section.

4.3.1 The effect of hydrogen loading time to writing time.

Figure 4.16 was shown the histogram of writing time at writing process for hydrogen loading time 72 hours with PMF fiber. The writing average did not high different from the writing time of the first experiment. Although, the average of writing time was better than the experiment result of the second experiment. Therefore, in case of hydrogen loading time unaffected to PMF fiber.

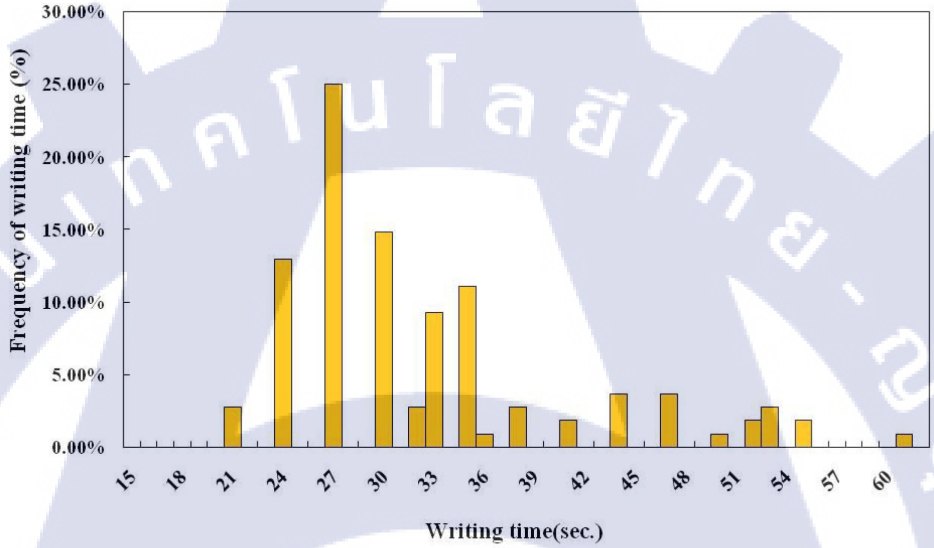

Figure 4.16 Histogram of writing time at writing process for hydrogen loading time 72 Hours

4.3.2 The effect of hydrogen loading time to FBG wavelength at optical inspection process.

Figure 4.17 was shown the histogram of FBG wavelength at optical inspection process for hydrogen loading time 72 hours with PMF fiber. The standard deviation of FBG wavelength in this condition were similar to the standard deviation of the first and the second experiments. It can verify that hydrogen loading time unaffected to FBG wavelength of PMF fiber.

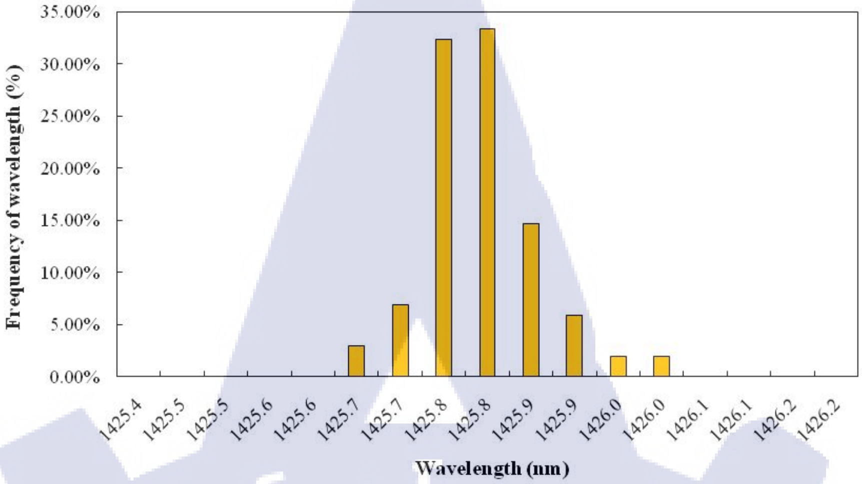

Figure 4.17 Histogram of FBG wavelength at optical inspection process for hydrogen loading time 72 Hours.

4.3.3 The effect of hydrogen loading time to Reflectivity

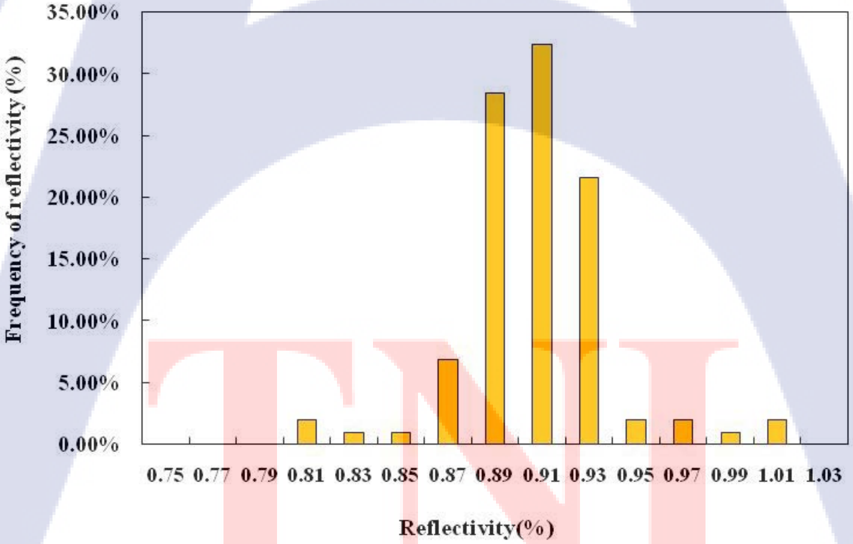

Figure 4.18 Histogram of reflectivity(%) at optical inspection process for hydrogen loading time 72 hours with PMF fiber.

Table 4.7 Statistical data of FBG parameter at different of hydrogen loading time for experiment 3

Parameters	Standard deviation	Specification of standard deviation	Judgment
Wavelengths (nm.)	0.061	0.12 nm	Accept
Reflectivity (%)	0.031	0.16 nm	Accept

Figure 4.18 was shown the histogram of reflectivity at optical inspection process for hydrogen loading time 72 hours with PMF fiber. The standard deviation of FBG wavelength in this condition were better than the standard deviation of the first and the second experiments. It can verify that hydrogen loading time unaffected to reflectivity of PMF fiber

4.3.4 Conclusion

Hydrogen loading time unaffected to FBG parameter of PMF fiber. The standard deviation of these parameter were considered to be the judgment factor.

Chapter 5

Conclusion and recommendation

The motivation of this research is to improve hydrogen loading time at hydrogen loading process for FBG fabrication productivity improvement. The objective of hydrogen loading process is to enhance photosensitivity in fiber. The photosensitivity reveal in term of writing time at writing process. The writing time is an important factor for FBG fabrication in case of cycle time and FBG quality. The side effect of hydrogen loading is refractive index of fiber core increasing. This lead to FBG wavelength shift to shorter wavelength when hydrogen gas diffuses from FBG. Therefore, hydrogen loading time is an important parameter to FBG fabrication. To improve hydrogen loading time, the effect of hydrogen concentration to FBG parameters are needed to study.

In this research was started from the evaluation of hydrogen loading concentration in fiber. The evaluation result found hydrogen concentration in fiber was proportional to hydrogen loading time. The equation to verify this relation was modified from the equation of Kazuhiro and teams. The modify equation to explain the relation of hydrogen concentration to hydrogen loading time was expressed by equation (5.1)

$$L = L_{sat}\left[1 - \exp(-\lambda_i^2 D_H (t - t_{cladding}) / b^2)\right] \tag{5.1}$$

The experiment result from hydrogen loss measurement was consistent well to hydrogen loss calculation in equation (5.1). This was effective for FBG fabrication to apply this equation to simulate hydrogen loss at various of hydrogen loading condition.

Writing time at writing process was the main parameter which effect from hydrogen loading time changing. Writing time was a reverse function of hydrogen loading time. The writing times of all hydrogen loading condition were accepted for FBG fabrication. The issue of writing time is long, it would handle by the power of

UV laser increasing. However, the increasing of power laser should concern to life time of the optics at writing process.

FBG wavelength was directly effect from hydrogen loading time. FBG wavelength is long when hydrogen loading time is long. However, the FBG wavelength will be shifted to shorter wavelength when hydrogen gas was eliminate from FBG. The standard deviation of all hydrogen loading condition were accepted for FBG fabrication. From the relation of hydrogen loss with hydrogen loading time in equation (5.1). The hydrogen loading time at 120 and 192 hours were mostly reach to the hydrogen loss at saturated value. The hydrogen loading time 42 and 72 were initial step of hydrogen loss penetration in to fiber. In this point should be inhomogeneous of hydrogen molecule in fiber. This lead to unstable of writing time and FBG wavelength at writing process.

FBG reflectivity and bandwidth were unaffected when hydrogen loading time changing. In case of reflectivity, the refractive index (Δn) and refractive index change from hydrogen ($n_{hydrogen}$) were eliminate by heat at FBG thermal stabilization and hydrogen annealing process. In case of bandwidth, the main effect of bandwidth was grating length.

The effect of hydrogen loading time to fiber type, there are two types of fiber in this research. Single mode fiber (SMF) and Polarization maintaining (PMF). From the test result, hydrogen loading time was unaffected to fiber type. This result was considered from the standard deviation of all FBG parameter.

These experiment result were scoped by hydrogen loading pressure at 13 MPa. FBG wavelength range at 980 nm and 1480 nm. FBG reflectivity at optical inspection process limit less than 4% and 1% for single mode fiber(SMF) and Polarization maintaining respectively.

References

References

[1] V. Alwayn, *Optical Network Design and Implementation*, San Jose: Cisco press, 2004.

[2] Ziemann, et, al., *Optical Short Rrange Transmission systems*, POF handbook: Springer, 2008.

[3] Technical University of Lodz, *"Fundamental of Optical Fiber Transmission,"* [Online]. Available: http: //www.mitr.p.lodz.pl/evu/lectures/Abramczyk1.pdf. [Accessed: October 11, 2015]

[4] K. O. Hill and G. Meltz, Fiber Bragg Grating Technology Fundamentals and Overview, *Journal of Lightwave Technology*, vol. 15, no.8, pp. 1263-1276, August 1997.

[5] M. M. Werneck, et al., *A Guide to Fiber Bragg Grating Sensors*, Brazil: InTech, 2013.

[6] R. Kashyap, *Fiber Bragg Grating*, Cannada : Academic Press, 1999.

[7] S. J. Mihailov, "Fiber bragg grating sensors for harsh environments," *Sensors 2012*, vol. 12, no. 2, pp. 1898-1918, February 2012.

[8] P. J. Lemaire, "Reliability of optical fibers exposed to hydrogen: prediction of long-term loss increases," *Optical Engineering*, vol. 30 no. 6, pp. 780-789, June 1991.

[9] K. Noguchi et al., "Loss increase for optical fibers exposed to hydrogen atmosphere," *Journal of Lightwave Technology*, vol. 3, no. 2, pp. 236-243, April 1985.

[10] Y. Masuda et al., "Wavelength evolution of fiber bragg gratings fabricated from hydrogen-loaded optical fiber during annealing", *Journal of Lightwave Technology*, vol. 22, no. 3, pp. 934-941, March 2004.

[11] P. L. Swart and A. A. Chtcherbakov, "Study of hydrogen diffusion in boron/germanium codoped optical fiber," *Journal of Lightwave Technology*, vol. 20, no. 11, pp. 1933-1941, November 2002.

[12] T. Erdogan et al., "Decay of UV-induce fiber Bragg gratings, *Journal of Applied Physics*, vol. 76, no. 1, pp. 73, March 1994.